ABSTRACT

Title of thesis: INTEGRATED ANALYSIS OF VERTICAL ALIGNMENTS AND SPEED PROFILES FOR RAIL TRANSIT ROUTES

Shu-Ta Yeh, Master of Science, 2003

Thesis directed by: Professor Paul M. Schonfeld
Department of Civil and Environmental Engineering

Frequent accelerations and decelerations for rail transit trains adversely affect in the major performance measures of travel time, tractive energy consumption and braking wear between stations. A dipped vertical alignment between rail transit stations provides trains some added advantages from gravity in accelerating as well as in decelerating.

A deterministic simulation model based on basic kinematics and resistance relations has been developed to compute train motions and energy consumption on specified vertical alignments. A baseline case study and the sensitivity of results to parameter changes are analyzed.

Vertical alignments and operating characteristics such as speeds and coasting distances are jointly optimized. Powell's Method is used for numerically optimizing total costs and other objective functions. Without speed constraints, the optimized total cost savings exceed 6.5%. The optimized alignment depths and total cost savings decrease as speeds are constrained to lower values.

The methods developed here may significantly improve rail transit systems.

INTEGRATED ANALYSIS OF VERTICAL ALIGNMENTS AND SPEED PROFILES FOR RAIL TRANSIT ROUTES

By

Shu-Ta Yeh

Thesis submitted to the Faculty of the Graduate School of the
University of Maryland, College Park in partial fulfillment
of the requirements for the degree of
Master of Science
2003

Advisory Committee:

Professor Paul M. Schonfeld, Chair
Professor Gang-Len Chang
Professor Kelly Clifton

ACKNOWLEDGEMENT

I would like to express my greatest appreciation to my advisor, Professor Paul Schonfeld, for his instruction and guidance for this research. Without his support, this thesis would not have been completed.

I am grateful to other members of my advisory committee, Professor Gang-Len Chang and Kelly Clifton, for their guidance and comments on this research.

TABLE OF CONTENTS

LIST OF TABLES

LIST OF FIGURES

Chapter 1. Introduction

1.1 Problem Statement

Rail transit systems are widely used to provide mass transportation in metropolitan areas. However, the frequent accelerations and decelerations for rail transit trains adversely affect in the major performance measures of travel time, propulsive energy consumption and braking wear between stations. If a dipped vertical track alignment between transit stations were applied, trains would take advantages from gravity in accelerating as well as in decelerating and reduce the disadvantages resulting from frequent accelerations and decelerations. With such a dipped transit track alignment, the following performance measures may be improved for a rail transit system:

1. Travel time between stations and related users' and supplier's costs.
2. Energy consumption for propulsion.
3. Braking wear and resulting maintenance costs.

However, providing such a dipped vertical track alignment may lead to the following problems:

1. Uncomfortable centrifugal acceleration in the vertical plane.
2. Gradients exceeding the maximum climbing ability of trains.
3. Increased construction cost.

Problem 1 constrains the rate of gradient change to satisfy standee comfort and safety requirements.

Problem 2 limits the maximum allowable gradient in order to start a train after an unexpected stop in a climbing section.

Problem 3 may be negligible when a deep tunnel is used between stations. However, if an elevated or cut-and-cover section is applied, the increased construction cost to build dipped vertical track alignments may be quite substantial.

1.2 Study Objectives and Scopes

The primary objectives of this research are (1) To develop a deterministic simulator with basic train kinematic relations and engineering equations for distinguishing transit trains movements on various vertical alignments and operating parameters. (2) To use it to evaluate rail transit operating performance measures with various track alignments. (3) To use Powell's Method and the deterministic simulator in optimizing alignments and operating characteristics.

In simulation experiments, one-directional train movements on vertical track alignments between stations will be investigated. The deterministic simulator will compute train movements using relations of vehicle kinetics, resistances, tractive effort, power, propulsive energy consumption, and braking energy consumption. The research will be focused on evaluating the relations between vertical alignment designs, travel time, tractive energy, braking energy and total costs.

A baseline simulation experiment will be introduced in chapter 4 and then repeated with various parameter changes for sensitivity analysis. This section will concentrate on (1) Generating simulation results of train travel time, propulsion fuel consumption, and brake wear under various operating options and vertical track alignments, and (2) Comparing and analyzing the effect of operating option changes under vertical track alignments.

Total costs functions are optimized in chapter 5 by using Powell's Method with the deterministic simulator. The optimized results may be provided to rail transit planners, designers and operators as new cost saving methods for the future network designs.

The major contributions different than previous studies are

1. Detailed baseline case study and sensitivity analysis to parameter changes.
2. Jointly optimization of vertical alignments and operating characteristics such as speeds and coasting distances

This thesis will proceed through the following steps:

1. Review of literature.
2. Descriptions of the deterministic simulation model, which includes the structure of the model, input variables and control rules.
3. Analysis of train performance measures of travel time, tractive energy consumption and braking wear between stations for various vertical track alignment designs with baseline parameters. After baseline analysis, a sensitivity analysis of changing in operating characteristics is investigated.
4. Optimizations of alignment designs and operating parameters.
5. Conclusions and recommendations.

Chapter 2. Literature Review

2.1 Relevant Studies

The use of a dipped alignment in a rail transit system has not been extensively analyzed in the literature. One published study on using dipped profiles in rail transit was done by Kim and Schonfeld (1997). They have created a deterministic simulation model to analyze rail transit train movement, energy consumption and braking consumption on a dipped vertical track alignment.

The vertical alignment used in this study is determined by two coefficients S, total parabolic curve length (which is equal to station spacing in this study), and δ, maximum depth halfway between two stations. The illustration and mathematical equations for that vertical alignment designs are shown in Figure 2.1

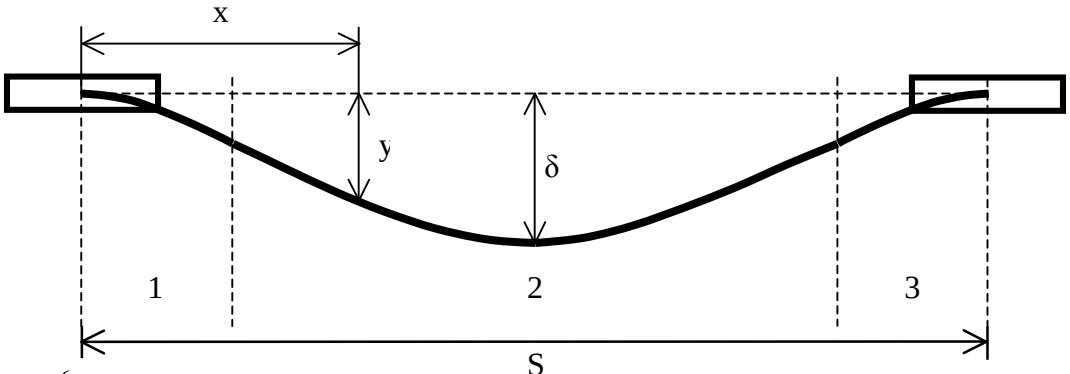

$$\begin{cases} y = \dfrac{-12\delta}{S^2} \cdot x^2 & for \quad 0 \le x < \dfrac{S}{6} \\ y = \dfrac{6\delta}{S^2} \cdot x^2 - \dfrac{6\delta}{S} \cdot x + \dfrac{\delta}{2} & for \quad \dfrac{S}{6} \le x < \dfrac{5S}{6} \\ y = \dfrac{-12\delta}{S^2} \cdot x^2 + \dfrac{24\delta}{S} \cdot x - 12\delta & for \quad \dfrac{5S}{6} \le x \le S \end{cases}$$

Figure 2.1 Dipped track profile used by Kim and Schonfeld (1997)

They have found that at the maximum allowable dip (using the maximum allowable gradient in alignments and a vertical dip halfway between stations equal to 1% of station spacing) the savings (compared with results on level track) exceed 9% for propulsive energy, 15% for braking energy, and 5% for travel time between rail transit stations. However, the previous study of Kim and Schonfeld has the following weaknesses:

1. The resistance equation used in the study is too old and the air resistance coefficient pertains to trains operating outside tunnels.
2. They assumed that the total parabolic curve length (one half-crest at both ends and one sag in the middle) is equal to station spacing. This assumption assumes no level platform section in either station and no level section in the middle between two stations.
3. No total cost analysis and optimization is conducted in this study. The results for travel time, tractive energy and braking energy consumption are analyzed separately, without being integrated and jointly optimized.

2.2 Studies in Cost Saving Models for Rail Transit System

Several studies have been found on reducing operation cost for rail transit systems. Uher and Sathi (1983) use the Energy Management Model, a series of computer simulation programs developed by the Rail System Center of Carnegie-Mellon University, to smooth the peak-power demand component of energy use. The reductions of the peak-power demand make it easier for a transit agency to negotiate the electricity rate and reduce the required facility investment.

Vuchic (1981) and Profillidis (1995) addressed electrodynamic braking (also known as regenerative braking) system in their books. While applying this system during braking, deceleration is obtained by converting the electric traction motors into electric generators. The power generated from train kinetic energy may be returned to the power network or simply be released by an electric resistor as heat in to the air.

The above two cost saving models can be used with dipped track profiles to take additional advantages from gravity in a rail transit system. However, due to the reduction in the required propulsive energy and braking energy for dipped track alignments, the additional cost savings from applying Energy Management Model or Regenerative Braking System together with dipped alignments will be lower than the additional cost savings from applying them with level tracks.

2.3 Kinetic and Empirical Engineering Equations

Vuchic's (1981) textbook emphasizes a systematic description of the basic concepts, terms, and relationships of urban public transportation. This book presents detailed descriptions and analyses of different transit modes, with emphases corresponding to their technical/operational complexities and their relative roles in urban transportation. Moreover, this book presents basic equations of vehicle motion, a description of the forces acting on the vehicle: resistance and propulsion, a definition of adhesion then leads to expressions for vehicle acceleration and stopping and diagrams and equations for computations of station-to-station travel times. Hay (1982) has illustrated rail-engineering

equations such as rail tractive force output equation, energy consumption equation and rail resistance equations in his publication. The equations provided by Vuchic and Hay will be used in the deterministic simulator design.

The American Railway Engineering Association (AREA) (1984) has provided almost all railway design guidelines used in current practice in its Manual for Railway Engineering. This manual requires that all changes in gradients should use vertical curve to connect and the length of a vertical curve is determined by the gradients to be connected. For high-speed main tracks, the rate of change should not be more than 0.05 % per station (of 100 ft) in sags and not more than 0.10 % per station in crest. For secondary main tracks, the rates of change may be twice those for high-speed main tracks. In 1926, W. J. Davis proposed an empirical formula for computing the " Tractive Resistance of Electric Locomotives and Cars" moving on straight and level track. However, the increased dimensions and heavier loading of fright cars, the much higher operating speeds of fright and passenger trains, and changes in the track structure have made it desirable to modify the constants in the Davis equation. The modified Davis Equation approved by AREA (1984) is shown in Equation 3.16.

Profillidis (1995) has provided train dynamic equations in his textbook. Various train traction and resistance relations developed and provided from organizations or agencies worldwide for various operating conditions are collected in this book. Section 12.2 of this book shows that the air resistance for trains operating in a tunnel with no openings is approximately three times the air resistance coefficient for a train running outside tunnels.

Wright and Ashford (1997) have provided vertical alignment design guidelines for railroads and rail transits. Railroad design is characterized by much smaller maximum grades and much longer vertical curves than are highways. The criterion for length of vertical curve is more critical for sags than for crests. Longer vertical curves are required for sag curves because of the tendency of undesirable slack to develop in the couplings as the cars in the front are slow down by the change of grade. Generally, much shorter curves are permitted along urban passenger rail lines than on mainline railroad tracks.

The Washington Metropolitan Area Transit Authority (WMATA) (2001) provides design criteria in architectural, civil, utility, structure, mechanical, electrical, train control and communications, systems and trackwork for its rail rapid transit system (METRORAIL). Parabolic vertical curves are required in rail transit alignment designs. The requirements of minimum vertical curve lengths are shown in Section 3.3. Vehicle characteristics and operating parameters to be used in WMATA METRORAIL system are also provided in this manual.

2.4 Railroad Simulation Models

Kikuchi (1991) has developed a simplified simulation model for the operational analysis of a rail rapid transit train. The model simulates the movement of a train along a route and develops the relations of time vs. distance, time vs. speed and distance vs. speed. It was found that the model could fairly accurately simulate the relations between travel time and distance.

Due to the presence of non-linear and complex phenomena, Minciardi et al. (1994) have suggested the use of discrete event simulations for train movement problems. They use two simulators to describe rail transit movements and energy consumption. The first is a simulator that allows the performance analysis of given schedule; the second is an integrated system simulator that allows the electrical analysis of the network during the movement of the train along the track.

Yu et al. (1994) have suggested an approach based on tabulated data to estimate traction motor efficiency. They use linear interpolation of an established data set to evaluate electric traction motors of a train moving at a specific speed and under a specific DC voltage.

Kim and Schonfeld (1997) have developed a deterministic transit train simulator to analyze train performance on a dipped alignment. The simulator can compute train movements with input parameters including vehicle characteristics, control options and track alignment then provide performance measures of train movement and propulsive and braking energy consumption.

2.5 Optimization of Total Cost

Vuchic's textbook (1981) provides cost components of various types of users' and supplier's costs for analyzing the total cost of a rail transit system. The components include 1. Capital cost: right-of-way acquisition, permanent way, stations, track superstructure, power supply, controls and communications, vehicle, maintenance and storage, engineering and administration and include operating and 2. Maintenance costs: transportation, permanent-way maintenance, vehicle maintenances, power, general and administrative. The total cost components to be used in this study are vehicle capital depreciation, power and maintenance cost and user in vehicle cost.

Press et al. (1989) present many algorithms, including Golden Section Search for one-dimensional optimization and Powell's Method for multi-dimensional optimization. Golden Section Search is a one-dimensional optimization method for minimizing an objective function that does not require pre-determined derivatives. It is also one bisection method developed to accelerate the convergence to optimized solutions. Powell's Method is used in this study for jointly optimizing multiple variables. With Powell's Method, one-dimensional optimizations (Golden Section Search in this study) for changing variables are repeatedly used until a combination of optimized values for which the objective function cannot be improved anymore is found.

Inose and Ishikawa (1994) compare civil engineering costs vs. tunnel depth showing that for shield tunneling (deep tunneling), construction cost is basically independent to tunnel depth for sites with good geology.

For the values used in total cost analysis, the Energy Information Administration (2003) provides statistical information about nationwide electric retail prices in the U.S. The information of electric retail prices can be used in calculating tractive energy expense. The American Public Transportation Association (2003) provides average new vehicle costs for heavy rail in the United States. The Washington Metropolitan Area Transit Authority (WMATA) (2002) provides operating statistics for its METRORAIL system within the fiscal year ending June 2002.

Chapter 3. Deterministic Simulation Model

The methodology used in this study is based on a deterministic simulation of train movements and energy consumption on a specified vertical track alignment for given control options. In this deterministic simulator, basic kinetic relations and experiential engineering equations are used to compute train movements and energy consumption. The results of travel time and energy consumption are included in a user and supplier cost function later to evaluate total effects of using dipped track alignment in a rail transit system.

3.1 Deterministic Simulation Model Assumptions

The following assumptions are considered in this deterministic simulation model:

1. The vertical track profile is symmetric about a central axis.
2. Parabolic curvatures are applied for the vertical curves while the gradient cannot exceed the maximum train climbing ability.
3. Horizontal curvatures are negligible for this analysis.
4. A concentrated mass is used to represent trains in motion.
5. A train accelerates with its full power unless it exceeds the comfort-limited acceleration.
6. The braking system can provide the maximum allowable comfort-limited deceleration rate.

7. A train starts cruising after reaching its cruising speed and begins coasting after passing a prespecified begin-coasting point.

Assumption 1 simplified the vertical alignment alternatives in this study. Based on this assumption, stations at both ends have to be equal in elevation.

Assumption 2 avoids rapid gradient change along the vertical alignment that may cause high centrifugal acceleration and reduce passenger comfort. In addition, a limitation of maximum gradient is required because a train may have to start without any moment on a climbing section.

Assumption 3 focuses this study only on the effects of vertical track alignments.

Assumption 4 assumes that the entire train mass can be considered as concentrated at one point. Assuming all cars located on the same point with the same gradient may cause some acceptable error.

Assumption 5 means that a train is assumed to use its full power to accelerate unless exceeding the comfort-limited acceleration.

Assumption 6 means that a train can always reach its maximum (comfort-limited) deceleration rate that is constrained by standee comfort and available adhesive force for a non-emergency condition.

Assumption 7 means that if cruising and coasting controls were applied in a simulation case, the start of cruising is controlled by train speed and the start of coasting is controlled by train position.

3.2 Structure of Deterministic Simulation Model

The structure of the deterministic simulator developed in this study consists of two parts:

The first part of this deterministic simulator is designed to find out when a train should start braking in order to stop precisely in the next station. A critical speed $v_{critical(x)}$ for a train in any point x between stations to start braking and stop precisely in the center of next station can be used to determine whether a train should brake or keep running. For any simulation step, if the train speed at its current location x exceeds the critical speed $v_{critical(x)}$, the train should brake in this simulation step. To create the relations of critical speed $v_{critical(x)}$ vs. position x , a small deterministic simulation that can analyze the movement from a stopped train to its previous stages is used here to determine the train dynamic during braking (Figure 3.1 is the critical speed analysis flow chart).

The second part is a deterministic simulation that can compute train movements, tractive energy consumption and braking energy consumption between two stations and then stop at a precise point in the arrival station (Figure 3.2 is the train motion analysis flow chart).

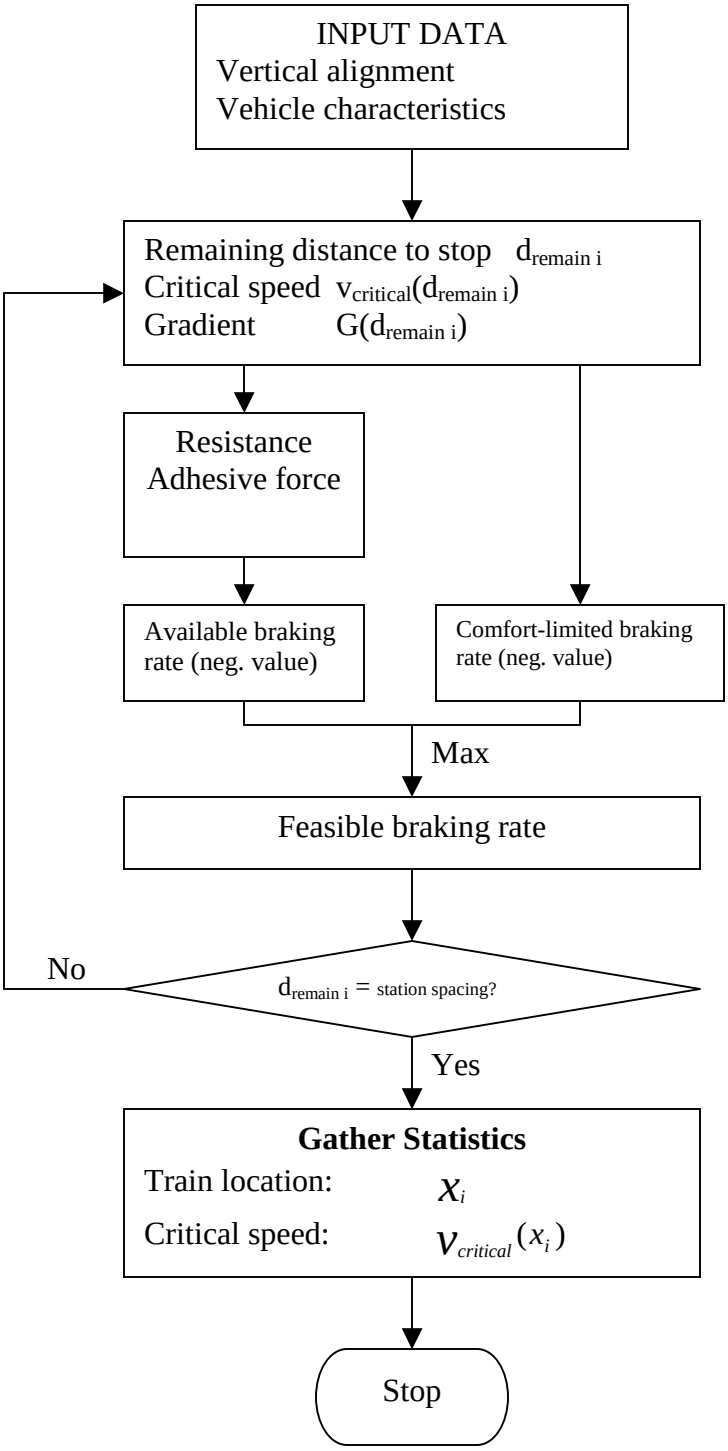

Figure 3.1 Flow chart of critical speed analysis

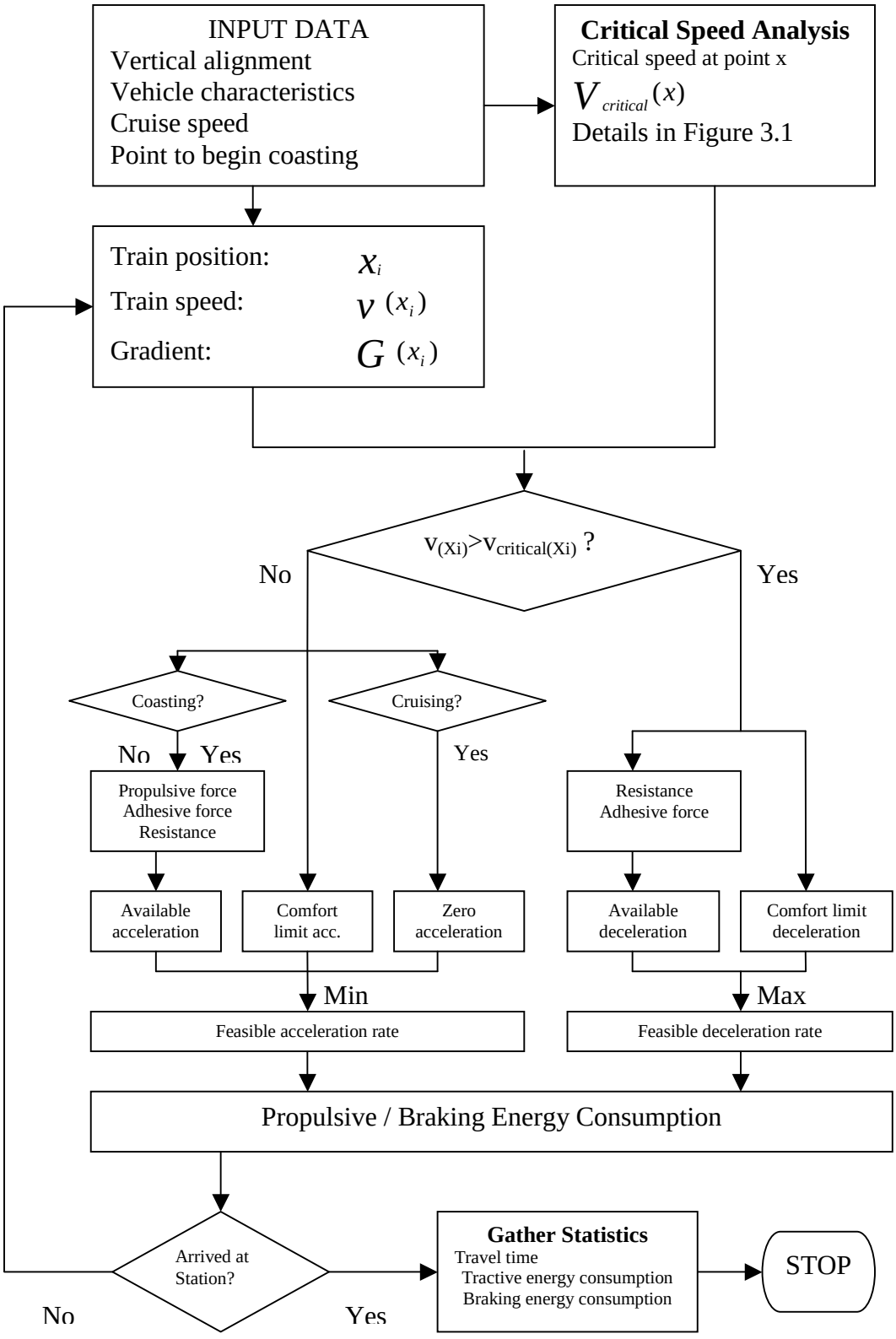

Figure 3.2 Flow chart of train motion analysis

3.3 Vertical Alignment Designs

The vertical track alignments used in this study are generalized from that suggested by Kim and Schonfeld (1997). As shown in Figure 3.3, sections I and VII are two level platform sections; sections II, III, V and VI are two crest and two sag parabolic vertical curves with coefficients S and δ in which S is the total length of the four parabolic curve sections and δ is the maximum depth of the vertical alignment; section IV is a level bottom section.

The mathematical functions for vertical track alignment are listed in Table 3.1 where L_j presents the length of section j and Δx_j, Δy_j are horizontal and vertical distances origin from the left end of section j; L_{pl} is the platform length; δ and S are coefficients for parabolic curves; L_{bt} is the level bottom length. The total station spacing L_{ss} in this vertical track alignment is $L_{pl} + S + L_{bt}$.

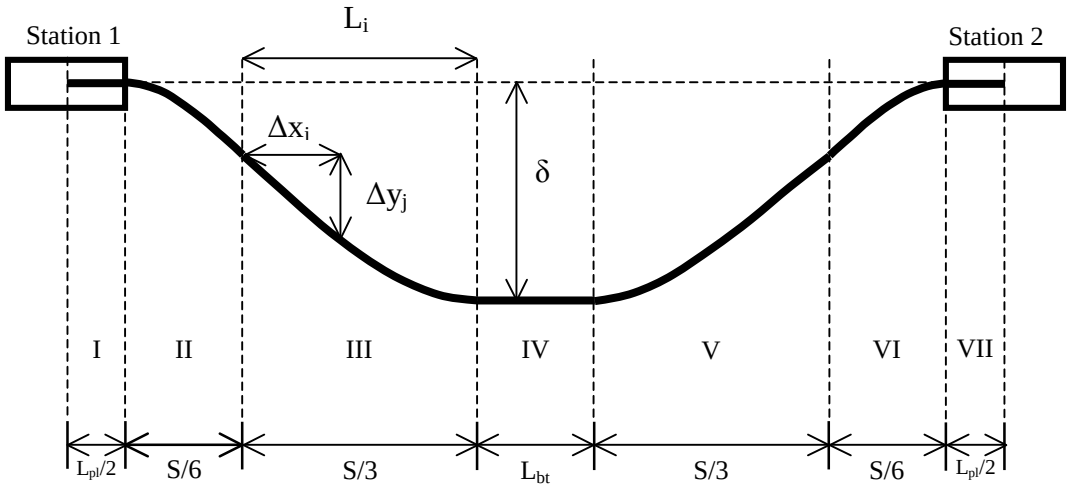

Figure 3.3 Vertical track alignments between stations

Table 3.1 Mathematical functions of vertical alignments

Section j	Length L_j	Elevation Δy_j	Tangent $\Delta y'_j$	Section description
I	$\frac{L_{pl}}{2}$	0	0	Departing platform
II	$\frac{S}{6}$	$\frac{-12\delta}{S^2}\cdot x_2^2$	$\frac{-24\delta}{S^2}\cdot x_2$	Descent crest
III	$\frac{S}{3}$	$\frac{6\delta}{S^2}\cdot x_3^2-\frac{4\delta}{S}\cdot x_3$	$\frac{12\delta}{S^2}\cdot x_3-\frac{4\delta}{S}$	Descent sag
IV	L_{bt}	0	0	Level bottom
V	$\frac{S}{3}$	$\frac{6\delta}{S^2}\cdot x_5^2$	$\frac{12\delta}{S^2}\cdot x_5$	Ascent sag
VI	$\frac{S}{6}$	$\frac{-12\delta}{S^2}\cdot x_6^2+\frac{4\delta}{S}\cdot x_6$	$\frac{-24\delta}{S^2}\cdot x_6+\frac{4\delta}{S}$	Ascent crest
VII	$\frac{L_{pl}}{2}$	0	0	Arriving platform

According to the design manual of WMATA (2001), the maximum gradient should not exceed ±4% for rail rapid transit tracks. In this study, the maximum gradient is 4δ/S and occurs at the end of section II and V. Therefore, the δ/S ratio in this study should not exceed 1% in any simulation case.

For the vertical curve length L_{vc}, WMATA requires that while operating within the 75mph speed constraint, the minimum length of vertical curve shall determined by the formula: $L_{vc} = (G_1-G_2)\ 100$

Where: L_{vc} = Length of curve, feet.

(G_1-G_2) = Algebraic difference of grades connected by the vertical curve, percent.

The absolute minimum length of vertical curve shall be 200 feet

According to WMATA's requirement, in this study, the formulation for minimum length requirement of vertical curvature with 75mph speed constraint can be rewritten with coefficients S and δ as

$$S > 24000 \times \frac{\delta}{S}$$

3.4 Mathematical Relations for Deterministic Simulation Model

The following mathematical relations are used to determine train movement and energy consumption in the deterministic simulator.

For any simulation step i, basic physical equations are applied for calculating train movement.

$$x_{i+1} = x_i + \Delta d_i = x_i + v_i \cdot \Delta t \qquad \left|\frac{x_i}{ft}\right|\left|\frac{v_i}{ft/s}\right|\left|\frac{\Delta d_i}{ft}\right|\left|\frac{\Delta t}{s}\right| \qquad (3.1)$$

$$v_{i+1} = v_i + \Delta v_i = v_i + a_i \cdot \Delta t \qquad \left|\frac{v_i}{ft/s}\right|\left|\frac{a_i}{ft/s^2}\right|\left|\frac{\Delta v_i}{ft/s}\right|\left|\frac{\Delta t}{s}\right| \qquad (3.2)$$

where x_i = train location at step i; v_i = train speed at step i; a_i = train acceleration/deceleration at step i; Δd_i = distance increment at step i; Δv_i = speed increment at step i; and Δt = time interval used in the deterministic simulation.

The main relation used to determine a train's acceleration is Newton's second law

$$a = \frac{F \cdot g}{m} \qquad \left|\frac{F}{lbw}\right|\left|\frac{g}{ft/s^2}\right|\left|\frac{m}{lb}\right| \qquad (3.3)$$

where a = acceleration; F = force (unit: lbw); g = the acceleration due to gravity; and m = mass of a body . Because the accelerating force for a train in motion is the difference between its available tractive effort $E_{available}$ and train resistance R_t, then available acceleration $a_{available}$ is

$$a_{available} = \frac{(E_{available} - R_t) \cdot g}{\rho \cdot m_t} \qquad \left|\frac{a_{available}}{ft/s^2}\right|\left|\frac{E_{available}}{lbw}\right|\left|\frac{R_t}{lbw}\right|\left|\frac{g}{ft/s^2}\right|\left|\frac{\rho}{-}\right|\left|\frac{m_t}{lb}\right| \qquad (3.4)$$

where ρ = coefficient for rotating masses(usually 1.04~1.10(Vuchic 1981)); m_t = train mass; R_t = train resistance

However, the available tractive effort $E_{available}$ is limited by both tractive force F_t and adhesive force F_a on driving wheels.

$$E_{available} = \min\{F_t, F_a\} \qquad \left|\frac{E_a}{lbw}\right|\left|\frac{F_t}{lbw}\right|\left|\frac{F_a}{lbw}\right| \tag{3.5}$$

The tractive force for rail vehicles is

$$F_t = \frac{375 \cdot \eta \cdot P}{V} \qquad \left|\frac{F_t}{lbw}\right|\left|\frac{\eta}{-}\right|\left|\frac{P}{Hp}\right|\left|\frac{V}{mile/h}\right| \tag{3.6}$$

where P = power; V = speed; η = transmission efficiency (typically 0.82 (Hay 1982)). Therefore, equation 3.6 can be rewritten as,

$$F_t = \frac{308 \cdot P}{V} \qquad \left|\frac{F_t}{lbw}\right|\left|\frac{P}{Hp}\right|\left|\frac{V}{mile/h}\right| \tag{3.7}$$

If a coasting operation (operating a train only with its moment, no traction from motors) is used for part of the travel between stations, the output tractive force should equal to zero during coasting operation.

The adhesive force for steel wheels on rail is

$$F_a = \mu \cdot F_n \qquad \left|\frac{F_a}{lbw}\right|\left|\frac{\mu}{-}\right|\left|\frac{F_n}{lbw}\right| \tag{3.8}$$

where F_n = normal force = the fraction of gravity force perpendicular to rail surface plus centrifugal force; μ = adhesive coefficient. Figure 3.22 of Vuchic's (1981) textbook shows that the relations between adhesive coefficient μ and train speed V for dry condition (in tunnel) are approximately equal to

$$\mu = 0.3 - 0.0015 \cdot 1.609 \cdot V \qquad \left|\frac{\mu}{-}\right|\left|\frac{V}{mile/h}\right| \tag{3.9}$$

$$F_n = \frac{m_t \cdot \left(g \cdot \cos\theta + a_{centrifugal}\right)}{g} \qquad \left|\frac{F_n}{lbw}\right|\left|\frac{m_t}{lb}\right|\left|\frac{g}{ft/s^2}\right|\left|\frac{\theta}{radian}\right|\left|\frac{a_{centrifugal}}{ft/s^2}\right| \tag{3.10}$$

$$\theta = \tan^{-1}\frac{G}{100} \qquad \left|\frac{\theta}{radian}\right|\left|\frac{G}{\%}\right| \tag{3.11}$$

where θ = angel from level; a_c = centrifugal acceleration; and G = percent of gradient.

Centrifugal acceleration can be expressed as follows:

$$a_{centrifugal} = \frac{v_i^{\,2}}{r_i} \qquad \left|\frac{a_{centrifugal}}{ft/s^2}\right|\left|\frac{v_i}{ft/s}\right|\left|\frac{r_i}{ft}\right| \tag{3.12}$$

$$r_i = \frac{\Delta d_i}{\Delta\theta_i} \qquad \left|\frac{r_i}{ft}\right|\left|\frac{\Delta d_i}{ft}\right|\left|\frac{\Delta\theta_i}{radian}\right| \tag{3.13}$$

$$\Delta d_i = \Delta t \cdot v_{i-1} \qquad \left|\frac{\Delta d_i}{ft}\right|\left|\frac{\Delta t}{s}\right|\left|\frac{v_i}{ft/s^2}\right| \tag{3.14}$$

$$\Delta\theta_i = \tan^{-1}\frac{G_i}{100} - \tan^{-1}\frac{G_{i-1}}{100} \qquad \left|\frac{\Delta\theta_i}{radian}\right|\left|\frac{G_i}{\%}\right| \tag{3.15}$$

where r_i = radius of vertical curvature at step i; and $\Delta\theta_i$ = angle change during step i-1 to i

In this study, train resistance is computed with the modified Davis Formula (AREA 1984). The unit resistance R_u (in pounds of force per short ton of vehicle weight) for a vehicle on a track without any horizontal curve is

$$R_u = 0.6 + \frac{20}{w} + 0.01 \cdot V + \frac{K \cdot V^2}{w n_a} + 20 \cdot G \qquad \left|\frac{R_u}{lbw/ton}\right|\left|\frac{w}{ton}\right|\left|\frac{V}{mile/h}\right|\left|\frac{K}{-}\right|\left|\frac{n_a}{-}\right|\left|\frac{G}{\%}\right| \tag{3.16}$$

where w = weight per axle in short tons; K = aerodynamic resistance coefficient; V = vehicle speed; and n_a = number of axles per vehicle. The total resistance of a vehicle is the vehicle weight W_v multiplied by its unit resistance R_u.

$$R_v = W_v \cdot R_u \qquad \left|\frac{R_v}{lbw}\right|\left|\frac{W_v}{ton}\right|\left|\frac{R_u}{lbw/ton}\right| \tag{3.17}$$

The total resistance of a train R_t is the summation of all individual vehicle resistances in a train. Thus, the total train resistance can be expressed as follows

$$R_t = \sum_{all\ \ v} R_v \qquad \left|\frac{R_t}{lbw}\right|\left|\frac{R_v}{lbw}\right| \tag{3.18}$$

For reasons of both safety and comfort to standees in a rail transit vehicle, it is necessary to limit the longitudinal acceleration and deceleration rate a (usually ±0.1~0.15g). The maximum allowable acceleration or deceleration rate is formulated as

$$-0.15 \cdot g \le a \le 0.15 \cdot g \qquad \left|\frac{g}{ft/s^2}\right|\left|\frac{a}{ft/s^2}\right| \tag{3.19}$$

where g = acceleration due to gravity.

Therefore, the maximum allowable acceleration rate a_{max} that can be used for a transit vehicle with standees is

$$a_{\max} \le 0.15 \cdot g \qquad \left|\frac{g}{ft/s^2}\right|\left|\frac{a_{\max}}{ft/s^2}\right| \tag{3.20}$$

An acceleration limit a_{cruise} used to prevent a train from exceeding the cruise speed in any simulation step is shown below

$$a_{cruise_i} = \frac{v_{cruise} - v_i}{\Delta t} \qquad \left|\frac{a_{cruise_i}}{ft/s^2}\right|\left|\frac{v_{cruise}}{ft/s}\right|\left|\frac{v_i}{ft/s}\right|\left|\frac{\Delta t}{s}\right| \tag{3.21}$$

where v_{cruise} = cruise speed; v_i = speed at step i; Δt = time interval used in simulation.

Therefore, the feasible acceleration rate $a_{feasible}$ can be expressed as

$$a_{\text{feasible}} = \min\left(a_{available}, a_{\max}, a_{cruise}\right) \quad \left|\frac{a_{\text{feasible}}}{ft/s^2}\right|\left|\frac{a_{available}}{ft/s^2}\right|\left|\frac{a_{\max}}{ft/s^2}\right|\left|\frac{a_{cruise}}{ft/s^2}\right| \tag{3.22}$$

For simulation steps during braking, the analysis process is very similar to steps used for accelerating. It was assumed earlier (Section 3.2) that the available braking force could reach the adhesive force limitation. Then the available braking rate $b_{available}$ is

$$b_{available} = -\left[\frac{(F_a + R_t)\cdot g}{\rho \cdot m_t}\right] \qquad \left|\frac{F_a}{lbw}\right|\left|\frac{R_t}{lbw}\right|\left|\frac{g}{ft/s^2}\right|\left|\frac{\rho}{-}\right|\left|\frac{m_t}{lb}\right| \tag{3.23}$$

The comfort-limited braking rate b_{min} is

$$b_{\min} \geq -0.15 \cdot g \qquad \left|\frac{g}{ft/s^2}\right|\left|\frac{b_{\min}}{ft/s^2}\right| \tag{3.24}$$

Therefore, the feasible deceleration rate $b_{feasible}$ can be expressed as ($b_{available}$ and b_{min} are negative values)

$$b_{\text{feasible}} = \max\left(b_{available}, b_{\min}\right) \quad \left|\frac{b_{\text{feasible}}}{ft/s^2}\right|\left|\frac{b_{available}}{ft/s^2}\right|\left|\frac{b_{\min}}{ft/s^2}\right| \tag{3.25}$$

For any specific point x between stations, a critical speed $v_{critical(x)}$ can be found from which a train can begin braking with full ability under non-emergency condition and stop precisely at the next station. These location-critical speed relations can be found by simulating backwards from a stopped train to its previous stages (see Figure 3.1). Whenever the critical speed vs. location table is

established, a 0-1 decision variable $Y_{braking(i)}$ for determining whether a train at simulation step i located at $_{Xi}$ with train speed $v_{(Xi)}$ should start braking can be specified as

$$\begin{cases} Y_{braking(i)} = 1, & v_{(Xi)} \geq v_{critical(Xi)} \\ Y_{braking(i)} = 0, & v_{(Xi)} < v_{critical(Xi)} \end{cases} \qquad \left| \frac{Y_{braking(i)}}{-} \right| \left| \frac{v_{(Xi)}}{ft/s} \right| \left| \frac{v_{critical(Xi)}}{ft/s} \right| \tag{3.26}$$

where $v_{(Xi)}$ = train speed at simulation step i and located at point $_{Xi}$; $v_{critical(Xi)}$ = critical speed at point $_{Xi}$; $Y_{braking(i)}$ = decision variables for a train to brake at simulation step i. If $Y_{braking(i)} = 1$, a train should brake at simulation step i.

Therefore, for any simulation step i, the applied train acceleration/deceleration rate $a_{applied}$ can be expressed as follows

$$a_{applied(i)} = \left(1 - Y_{braking(i)}\right) \cdot a_{\text{feasible}(i)} + Y_{braking(i)} \cdot b_{\text{feasible}(i)}$$
$$\left| \frac{a_{applied(i)}}{ft/s^2} \right| \left| \frac{Y_{braking(i)}}{-} \right| \left| \frac{a_{\text{feasible}(i)}}{ft/s^2} \right| \left| \frac{b_{\text{feasible}(i)}}{ft/s^2} \right| \tag{3.27}$$

Energy consumption

Once the applied train acceleration/deceleration rate is determined, the applied tractive effort $E_{applied}$ can be computed as

$$E_{applied} = R_t + a_{applied} \cdot \rho \cdot m_t \qquad \left| \frac{E_{applied}}{lbw} \right| \left| \frac{a_{applied}}{ft/s^2} \right| \left| \frac{\rho}{-} \right| \left| \frac{m_t}{lb} \right| \tag{3.28}$$

If $E_{applied}$ is positive, some tractive force from motors is required. If $E_{applied}$ is negative, some drag force from braking system is required.

The applied power $P_{applied}$ used for generating the applied tractive effort $E_{applied}$ is

$$P_{applied} = \frac{E_{applied} \cdot V}{308} \qquad \left|\frac{P_{applied}}{hp}\right| \left|\frac{E_{applied}}{lbw}\right| \left|\frac{V}{mile/h}\right| \tag{3.29}$$

The energy consumption Δe within time interval Δt is

$$\Delta e = P_{applied} \cdot \frac{\Delta t}{3600} \cdot \frac{1}{1.341} \qquad \left|\frac{\Delta e}{kwh}\right| \left|\frac{P_{applied}}{hp}\right| \left|\frac{\Delta t}{s}\right| \tag{3.30}$$

If energy consumption "Δe" is positive, some tractive energy consumption is recorded for this step. If a negative "Δe" value is found here, braking energy consumption is recorded.

Microsoft Excel 2000 is used in this study to compute train movements and energy consumption. For any data row i (simulation step i) in the spreadsheet, the performance measures of travel time, tractive energy consumption and braking wear between stations will be calculated with the processing flow as in Figures 3.1 and 3.2 with above mathematical relations. The major advantage for using spreadsheet in the calculation is that information for all simulation steps are stored and are easy to review train performance for any specific simulation steps. The disadvantage for using spreadsheet is that the computing time will be longer. The selected time interval used in the deterministic simulator is 0.01 second.

3.5 Total Cost Evaluation

In this study, the cost evaluation focus on costs for a one-directional operation between two stations. Thus, the part for user cost is user-in-vehicle cost. The supplier costs are the vehicle capital expenses (vehicle depreciation), energy expenses (energy consumption) and braking wear expenses plus the averaged construction cost for a one-directional operation between stations. The formulas for total cost between stations are

$$C_t = C_u + C_s \qquad \left|\frac{C_t}{\$}\right|\left|\frac{C_u}{\$}\right|\left|\frac{C_s}{\$}\right| \tag{3.31}$$

$$C_u = T \cdot n_c \cdot N_p \cdot v_{user} \qquad \left|\frac{C_u}{\$}\right|\left|\frac{T}{hr}\right|\left|\frac{n_c}{car/train}\right|\left|\frac{n_p}{psg/car}\right|\left|\frac{v_{user}}{\$/psg-hr}\right| \tag{3.32}$$

$$C_s = n_c \cdot T \cdot v_{vehicle} + E_t \cdot v_{tractive} + E_b \cdot v_{braking} + C_{construction}$$

$$\left|\frac{C_s}{\$}\right|\left|\frac{n_c}{-}\right|\left|\frac{T}{hr}\right|\left|\frac{v_{vehicle}}{\$/vehicle-hr}\right|\left|\frac{E_t}{kwh}\right|\left|\frac{v_{tractive}}{\$/kwh}\right|\left|\frac{E_b}{kwh}\right|\left|\frac{v_{braking}}{\$/kwh}\right|\left|\frac{C_{construction}}{\$}\right| \tag{3.33}$$

where C_t = total cost for a one-directional operation; C_u = user cost; C_s = supplier cost; T = travel time between stations; n_c = number of cars per train; n_p = number of passengers per car; v_{user} = average in vehicle time value per passenger; $v_{vehicle}$ = vehicle depreciation per revenue hour; E_t = tractive energy consumption; $v_{tractive}$ = unit tractive energy cost; E_b = braking energy consumption; $v_{braking}$ = unit braking energy cost; $C_{construction}$ = averaged construction cost for a one-directional operation between stations.

3.6 Description of Train Simulator Output

After completing the calculation, the deterministic simulator is required to produce the following results

1. Overall statistical information

This part of report includes the statistics for a one-directional operation between stations. The results contain

a. Review of input parameters:

Track alignment, vehicle characteristics and operation options.

b. Major performance measures:

Total travel time; tractive energy consumption; and braking consumption.

c. Cost components:

Users-in-vehicle cost, vehicle capital expense, propulsive energy cost, braking cost and total cost

d. Special event descriptions

Points of begin cruising, coasting, and braking; maximum speed and first point to reach it; maximum and minimum centrifugal acceleration.

2. Position-sorted and time-sorted simulation profiles

Performance profiles between stations are provided in this part of reports. The profile data are sorted by either train locations or simulation times for the purpose of comparing and analyzing results between simulation cases. The information in performance profiles includes train location, travel time, speed, depth, gradient, tractive effort, resistance, applied acceleration, tractive energy and braking energy consumption and accumulation.

Chapter 4. Evaluation of Results

4.1 Comparison with Previous Model Results

Numerical results from the deterministic simulator developed in this study were compared with results in Kim and Schonfeld's (1997) study. A modified train deterministic simulator using the same train resistance and engineering equations as Kim and Schonfeld's is developed to check the accuracy of the deterministic simulator used in this study.

Table 3.2 shows comparison of results with the same inputs into simulators developed in this study and in Kim and Schonfeld's study. The results show that the simulation model developed in this study is equivalent to the one developed by Kim and Schonfeld. The discrepancies between results may due to the selection of units. English units are used for simulator in this study while Kim and Schonfeld used SI units in their simulator.

Table 4.1 Comparison with previous model results

Baseline Assumptions Station Spacing: 3000m Max acceleration: 1.3m/s^2 Car power: 520 kw/car Unconstrained speed Car weight: 40 ton		Travel Time (Sec.)		Tractive Energy (KWH)		Braking Energy (KWH)	
		Kim & Schonfeld	Yeh	Kim & Schonfeld	Yeh	Kim & Schonfeld	Yeh
0% Dip	Baseline	119.0	118.8	75.6	73.9	58.5	57.2
	Acc.: 1.0 m/s^2	125.7	125.3	72.1	71.1	56.3	55.0
	Pow.: 416 KW	125.5	125.4	66.9	65.8	50.9	50.4
	Spd.: 120 km/hr	122.7	122.8	57.1	56.7	40.8	41.2
0.5% Dip	Baseline	114.7	114.6	71.9	70.8	53.6	52.9
	Acc.: 1.0 m/s^2	121.4	121.3	67.8	67.0	51.1	49.8
	Pow.: 416 KW	120.4	120.0	63.4	62.6	46.2	46.1
	Spd.: 120 km/hr	120.5	120.8	55.1	54.5	38.3	38.7
1% Dip	Baseline	113.5	111.0	68.5	67.7	49.3	48.7
	Acc.: 1.0 m/s^2	118.6	117.7	63.8	63.0	46.1	44.7
	Pow.: 416 KW	121.7	115.9	60.2	59.7	42.6	42.0
	Spd.: 120 km/hr	119.5	118.9	55.1	54.5	35.2	38.4

4.2 Baseline Case Assumptions

The simulation is conducted for baseline operating parameters with various vertical alignments and then, repeated with certain parameter changes for sensitivity analysis.

The evaluations of simulation results in this section focus on the analysis of baseline cases with specified parameters of vehicle characteristics, control parameters and station spacing under various vertical alignments. The design parameters used in this baseline evaluation are listed in Table 4.2. The numeral assumptions for vehicle characteristic and control options are generated from the values given by WMATA (2001) manual of design criteria. A high air resistance coefficient is used because Profillidis (1997) suggests that the air resistance coefficient for a train running in a tunnel with no openings is approximately three times the air resistance coefficient for a train outside tunnels.

Table 4.2 Parameters used in baseline cases

	Parameters	Value	Units
Alignment	Station spacing L_{ss}	12500	Feet
	Platform length L_{pl}	500	Feet
	Total curve length S	Variable	Feet
	Maximum depth δ	Variable	Feet
	Level bottom length L_{bt}	Variable	Feet
Simulation Assumptions	Car power	520	KW
	Car weight	50	Ton
	Powered-axle/ Axle per car	4/4	-
	Number of cars per train	6	-
	Comfort-limited acceleration	4.827 (0.15g)	ft/s^2
	Cruise speed	Unconstrained	ft/s^2
	Coasting distance	No coasting	Feet
	Air resistance coefficient	As in tunnels	-

Within baseline station spacing (12,500 ft), various alignment designs with combinations of parabolic curve coefficients S and δ are analyzed. According to the definition of S and δ from Section 3.4, total curve length S should be smaller or equal to total station spacing minus length of platform and δ/S ratio should not exceed 1%. The illustrations of vertical alignment designs with 12,500 feet station spacing are shown in Figure 4.1. Operating on alignments with relatively short curves, trains will dive to the lowest elevation in a short distance and then keep operating in the level section until they reach the climbing curves. However, due to the 1% constraint of δ/S ratio, alignments with short curves cannot have depths greater than 0.01S.

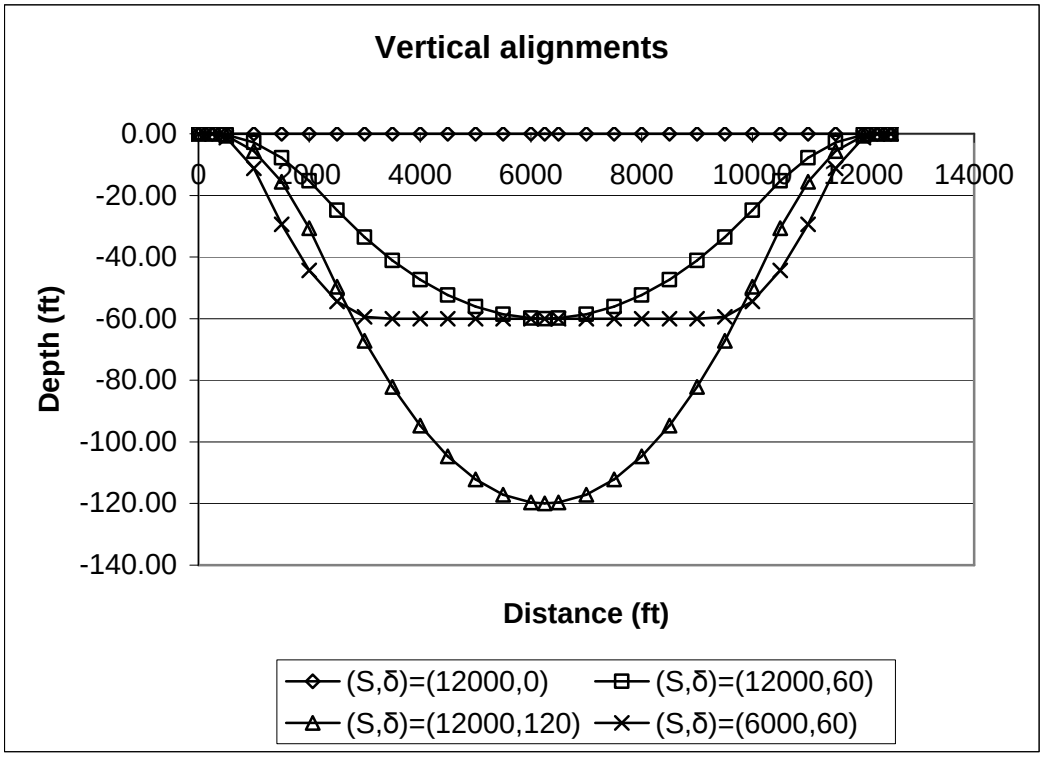

Figure 4.1 Illustrations of vertical alignments

4.3 Major Performance Measures Comparison of Baseline Cases

27 vertical alignment designs with baseline operating parameters have been calculated in this section. The results for travel time T, cumulative tractive energy consumption E_t and cumulative braking energy consumption E_b for the cases with various alignment designs are listed in Table 4.3.

Table 4.3 Simulation results with baseline parameters

		Total Parabolic Curve Length S (ft)											
Max. Depth δ (ft)		2000		4000		6000		8000		10000		12000	
		Profile	%*	Profile	%*	Profile	%*	Profile	%*	Profile	%*	Profile	%*
0	T (sec)	149.46	0.00	149.46	0.00	149.46	0.00	149.46	0.00	149.46	0.00	149.46	0.00
	E_t (kwh)	106.48	0.00	106.48	0.00	106.48	0.00	106.48	0.00	106.48	0.00	106.48	0.00
	E_b (kwh)	58.82	0.00	58.82	0.00	58.82	0.00	58.82	0.00	58.82	0.00	58.82	0.00
20	T (sec)	146.10	-2.24	146.22	-2.16	146.87	-1.73	147.40	-1.38	147.29	-1.45	147.72	-1.16
	E_t (kwh)	103.36	-2.93	104.10	-2.23	104.61	-1.75	104.92	-1.47	105.15	-1.25	105.34	-1.07
	E_b (kwh)	54.04	-8.12	54.63	-7.11	55.23	-6.10	55.67	-5.35	56.01	-4.77	56.38	-4.13
40	T (sec)			143.47	-4.01	144.37	-3.40	144.65	-3.22	145.22	-2.84	145.68	-2.53
	E_t (kwh)			101.72	-4.47	102.79	-3.47	103.48	-2.82	103.94	-2.39	104.31	-2.05
	E_b (kwh)			50.40	-14.32	51.60	-12.26	52.51	-10.72	53.27	-9.43	53.96	-8.26
60	T (sec)					141.50	-5.33	142.42	-4.71	143.23	-4.17	144.04	-3.63
	E_t (kwh)					101.02	-5.13	102.12	-4.10	102.81	-3.45	103.35	-2.95
	E_b (kwh)					47.92	-18.53	49.42	-15.97	50.58	-14.00	51.63	-12.22
80	T (sec)							140.38	-6.07	141.51	-5.32	142.48	-4.67
	E_t (kwh)							100.85	-5.29	101.77	-4.43	102.47	-3.77
	E_b (kwh)							46.39	-21.13	47.97	-18.45	49.35	-16.10
100	T (sec)									140.06	-6.29	141.18	-5.54
	E_t (kwh)									100.80	-5.33	101.65	-4.54
	E_b (kwh)									45.41	-22.79	47.13	-19.87
120	T (sec)											139.69	-6.53
	E_t (kwh)											100.91	-5.23
	E_b (kwh)											44.92	-23.62

T: Travel time E_t: Tractive energy consumption E_b: Braking energy consumption

%* : Percentage Saving (compared to results of level track)

Figures 4.2 to 4.4 show relations between major performance measures of travel time, tractive energy consumption and braking wear between stations and various alignment designs. Compared with results of level track, the deepest alignment (S=12000 ft; δ=120 ft) has the greatest saving in travel time, tractive energy and braking energy. The maximum saving rates are 6.53% in travel time, 5.23% in tractive energy and 23.62% in braking energy. In addition, the saving for cases with the same total curve length S but different in maximum depth δ are approximately proportional to the value of δ. Moreover, when comparing results from cases with the same maximum depth δ, cases with shorter total parabolic curves S (trains dive to the lowest points in a shorter distance) have greater savings in travel time, tractive energy and braking energy.

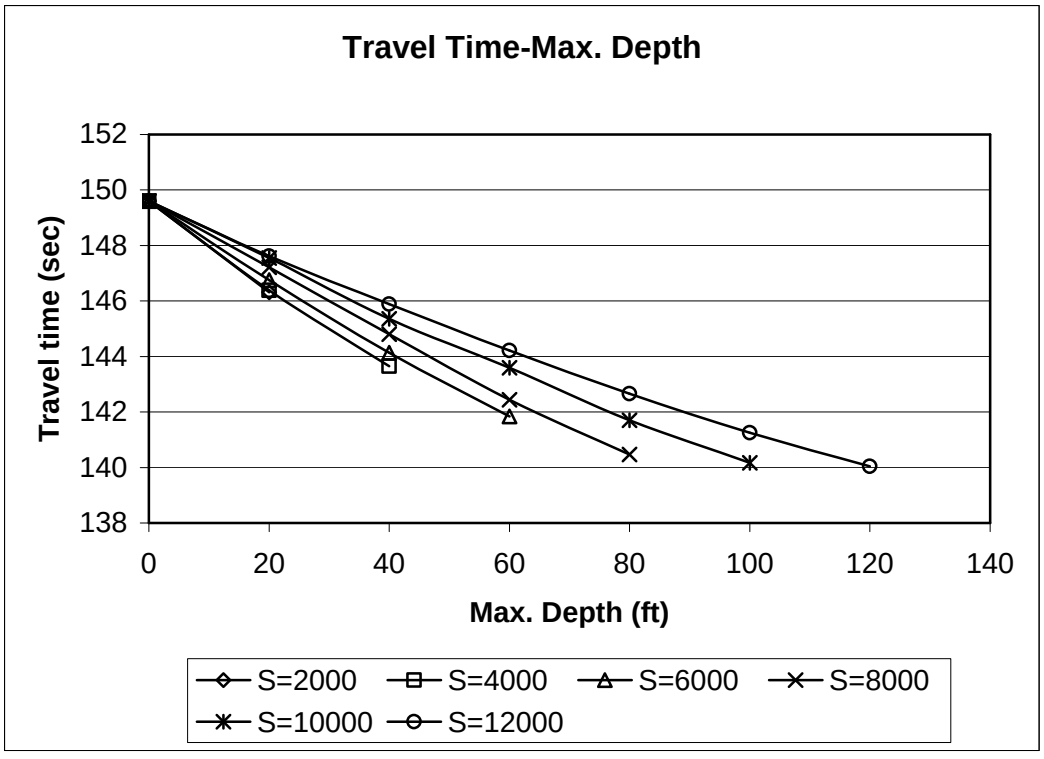

Figure 4.2 Travel time-Maximum depth relations

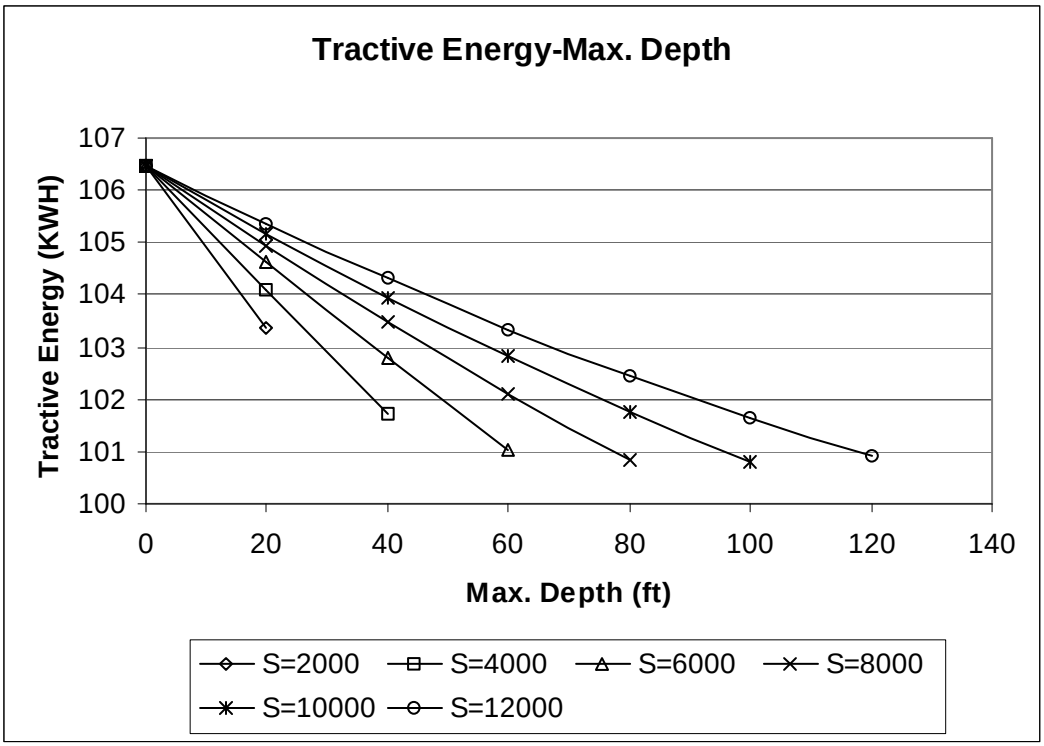

Figure 4.3 Tractive Energy-Maximum depth relations

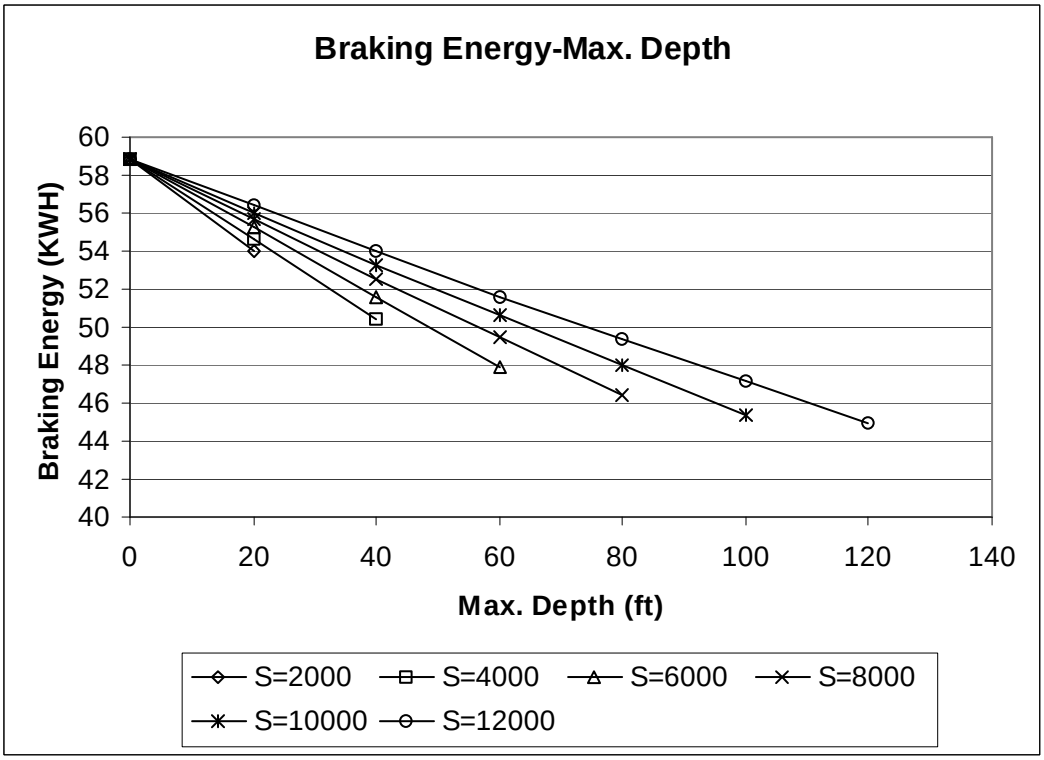

Figure 4.4 Braking energy-Maximum depth relations

4.4 Performance Profile Comparison

Performance profiles between four selected alignment designs (Table 4.4; Figure 4.1) with baseline assumptions are discussed in this section. In addition, the selected baseline cases were classified into two sets based on two concepts. The first set of cases includes cases 1, 2, and 3 whose vertical alignments have the same total curve length S (12000 ft) but different maximum depths δ (0 ft; 60 ft; 120 ft). The second set of cases includes cases 1, 2, and 4, which contain one level track and two dipped alignments with the same value in maximum depth δ (60ft) but different values of total curve length S (6000ft; 12000ft).

Table 4.4 Selected baseline cases for simulation profile comparison.

Cases	Total curve length S (ft)	Maximum depth δ (ft)	δ / S ratio
1	-	0	0%
2	12000	60	0.5%
3	12000	120	1%
4	6000	60	1%

For performance profiles of each selected baseline case, location-sorted and time-sorted profile are provided here. The reason for using a location-sorted data is to observe and compare train movements under related geographic conditions between alignments. The reason for using time-sorted data is to observe and compare time-related information.

4.4.1 Performance Profile Comparison for Case Set 1

The first case set contains three alignments with the same total curve length S but different maximum depth δ (0 ft; 60 ft; 120 ft). In this set of baseline cases, the savings for travel time, tractive energy and braking energy are listed in Table 4.5. For baseline cases in set 1, the savings in travel time, tractive energy and braking are approximately proportional to the value of maximum depth δ.

Table 4.5 Travel time, tractive energy and braking energy for baseline case set 1

	Case1 (S=12000; δ=0)		Case 2 (S=12000; δ=60)		Case 3 (S=12000; δ=120)	
	Result	Saving*	Result	Saving*	Result	Saving*
Travel Time (sec)	149.46	0%	144.04	-3.63%	139.69	-6.54%
Tractive E. (kwh)	106.48	0%	103.35	-2.94%	100.91	-5.23%
Braking E. (kwh)	58.82	0%	51.63	-12.22%	44.92	-23.63%

Saving* is the difference in percentage compared to results of level track

Figures 4.5 and 4.6 show the relations between train locations and their elevation or gradient. The case with larger maximum depth δ has greater change in both elevation and gradient.

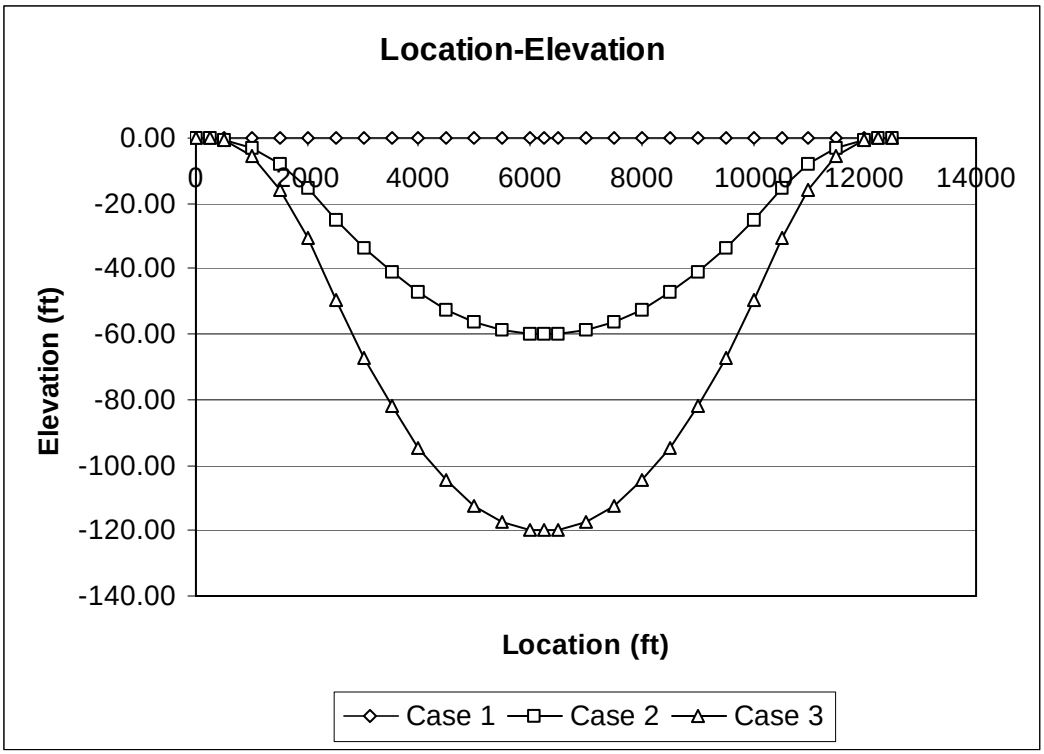

Figure 4.5 Location-Elevation relations for baseline case set 1

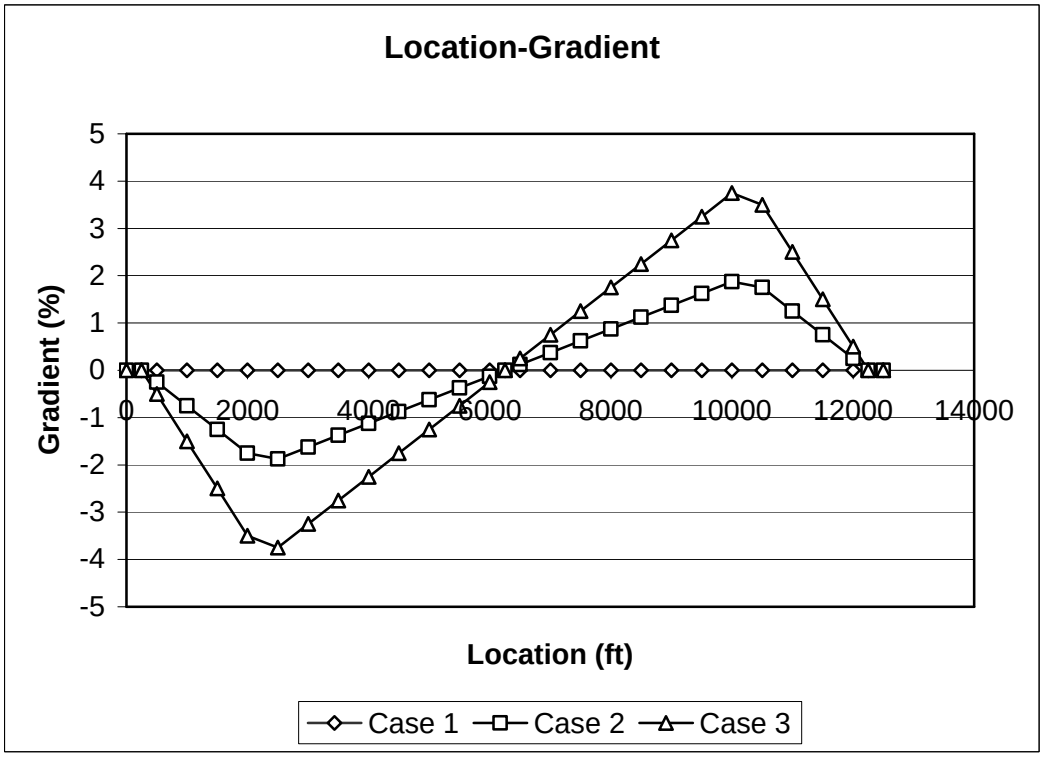

Figure 4.6 Location-Gradient relations for baseline case set 1

Figure 4.7 is the location-resistance diagram. For trains operating on dipped alignments, the train resistances are affected rapidly by the changes of gradient.

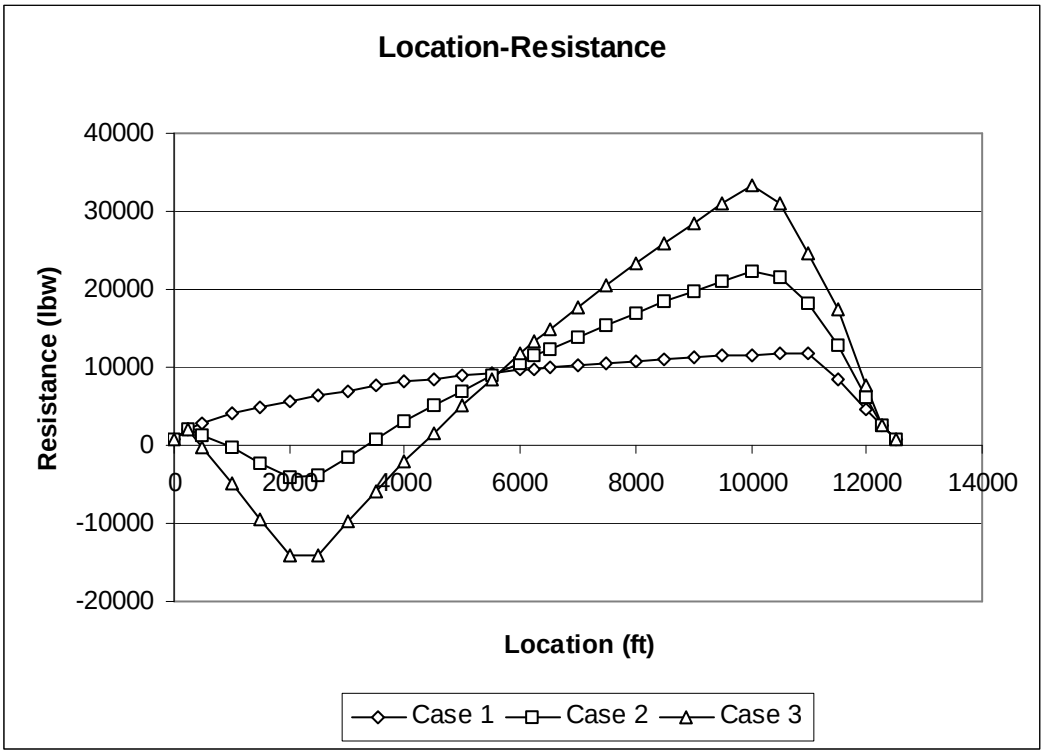

Figure 4.7 Location-Resistance relations for baseline case set 1

Figure 4.8 is the location-acceleration diagram. On a dipped alignment, due to the low resistance in the first half (0~6250 ft), descending trains can operate with slightly higher acceleration rate than trains on level track.

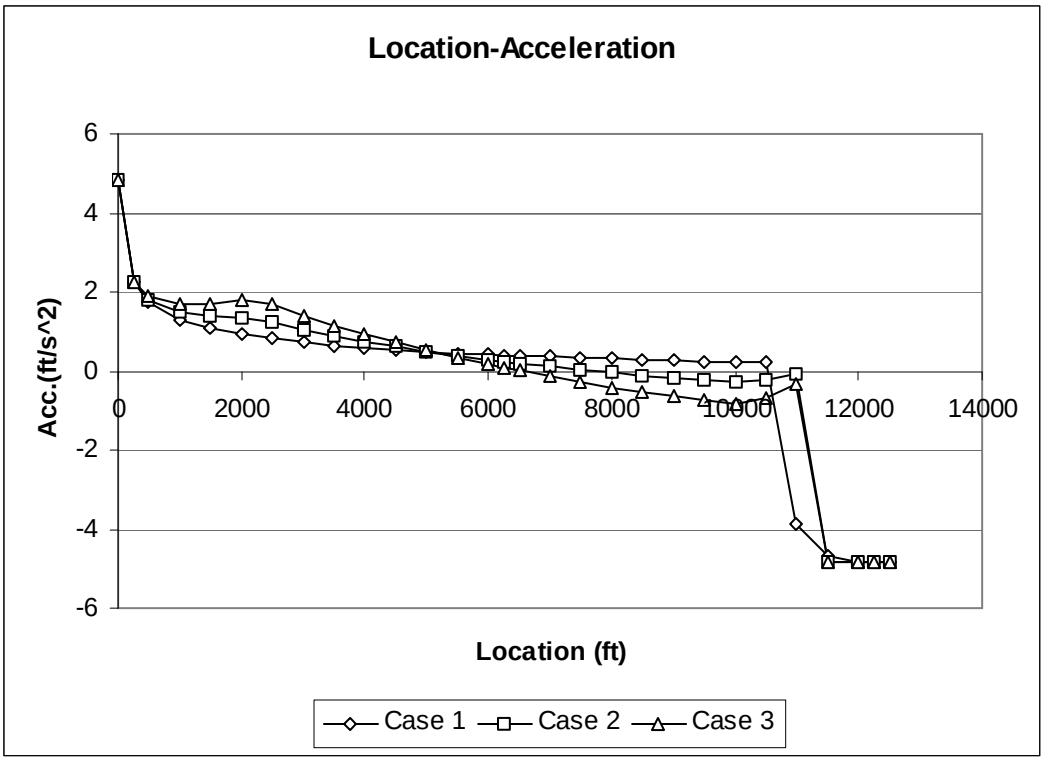

Figure 4.8 Location-Acceleration relations for baseline case set 1

Figures 4.9 and 4.10 show location-speed and location-time relations. The speed gaps between case 1, case 2 and case 3 increase with the train movements in the descending section (first half). In the climbing section (second half), the train speed gaps between cases decrease with the train movements. The greatest speed differences between the three cases occur around halfway between stations (lowest points for dipped alignments). Due to high operating speeds, travel times between stations are short for dipped alignments.

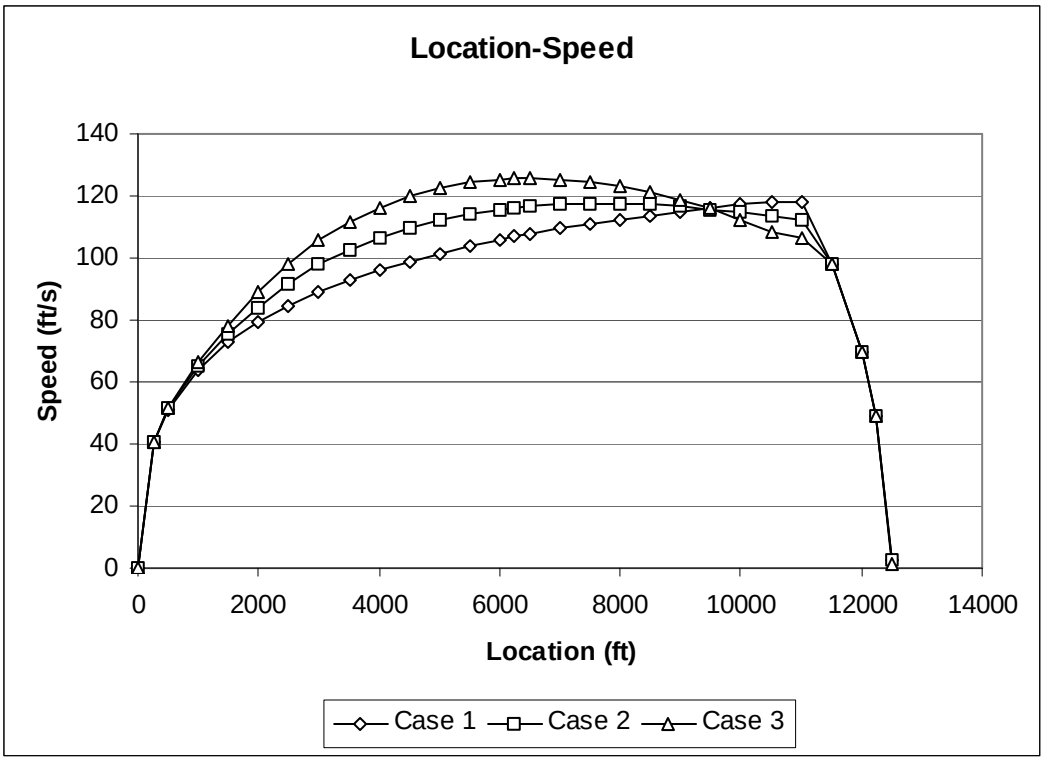

Figure 4.9 Location-Speed relations for baseline case set 1

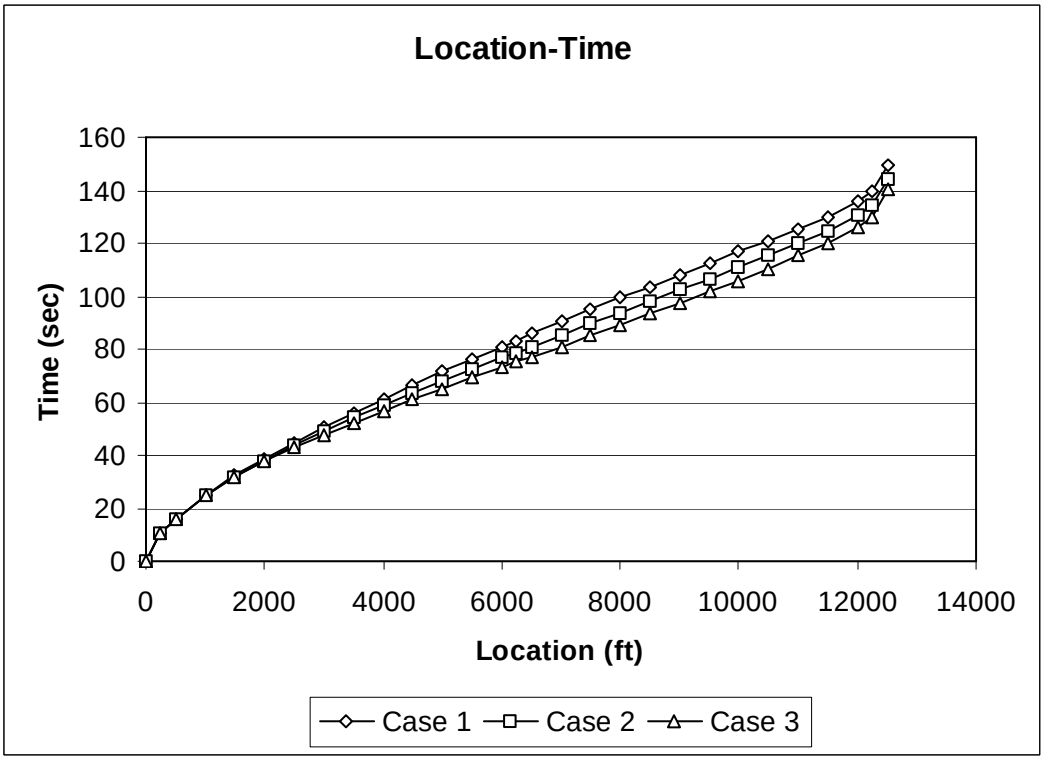

Figure 4.10 Location-Time relations for baseline case set 1

Figure 4.11 is the time-acceleration diagram. This figure shows that after 4 seconds (approximately 40 feet in travel distance) the traction motors cannot provide acceleration higher than comfort-limited acceleration (0.15g). After that, the acceleration rates for three cases are influenced by the gradient.

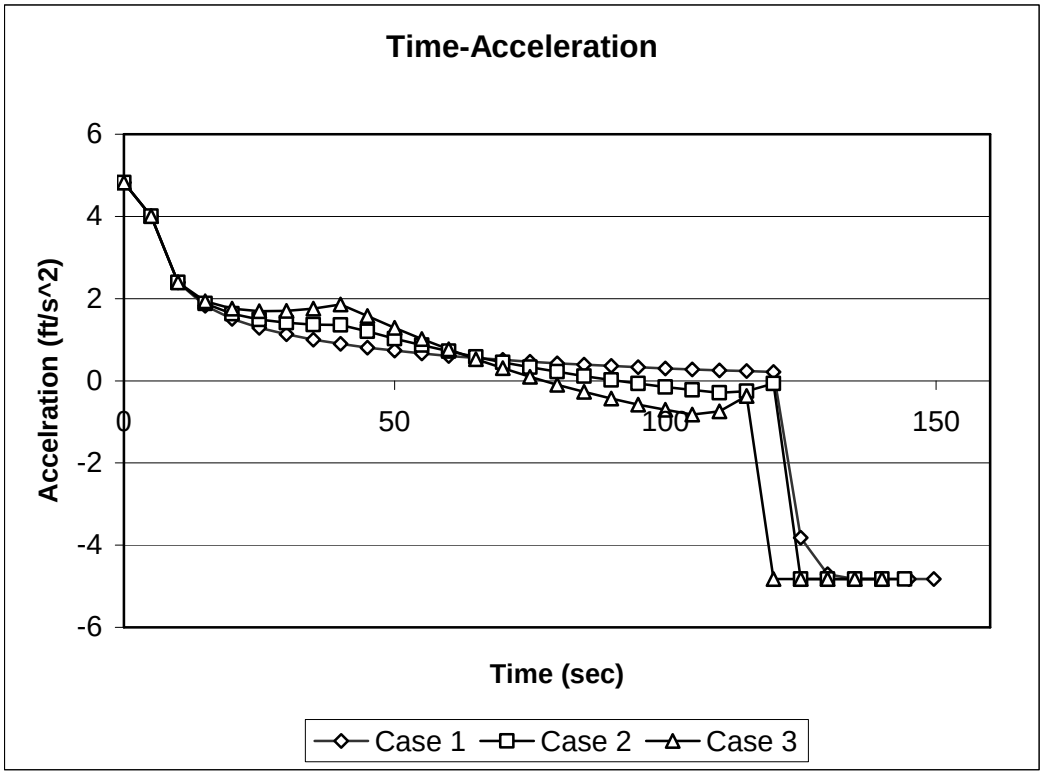

Figure 4.11 Time-Acceleration relations for baseline case set 1

Figure 4.12 shows the relations between time and speed. The areas under trajectory lines are total station spacing. Because the station spacing for the three baseline cases are equal, the trajectory line with higher peak value (speed) can reach the x-axis faster (trains arrive next station in shorter time).

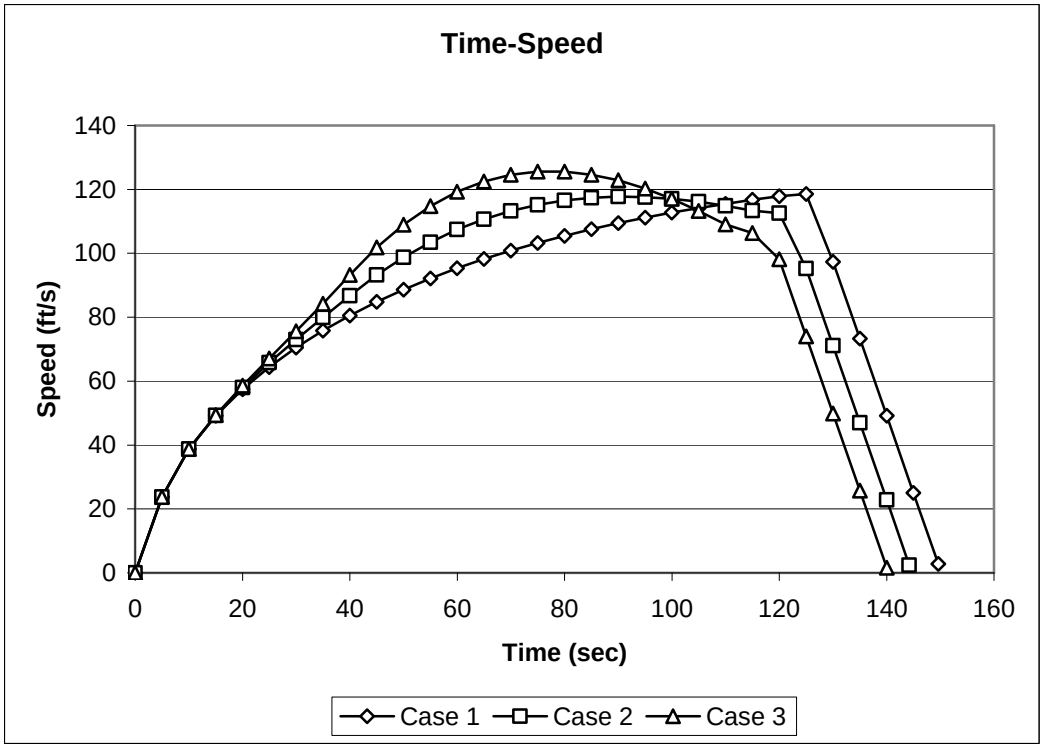

Figure 4.12 Time-Speed relations for baseline case set 1

Figure 4.13 shows the relations between time and cumulative tractive energy. Because no speed constraints are applied in baseline study, trains in all cases operate with their full power until starting to brake. Thus, the energy consumption per unit time is equal for trains in all cases and trains start braking earlier consume less tractive energy between stations.

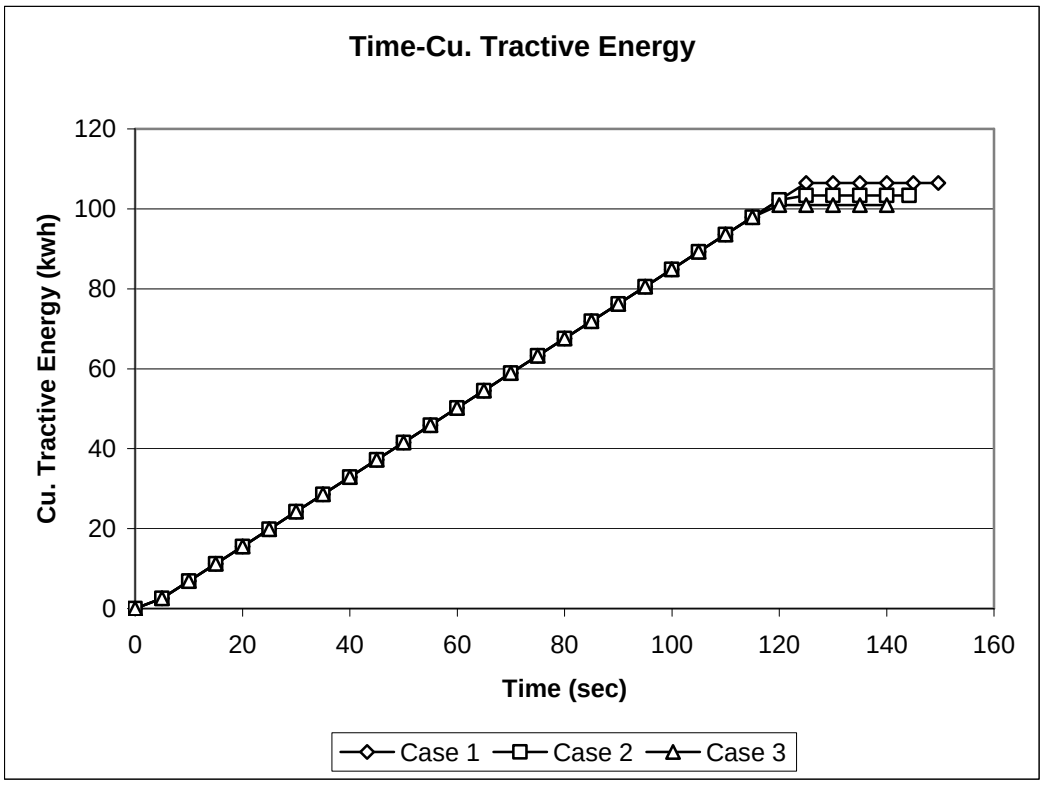

Figure 4.13 Time-Cumulative tractive energy relations for baseline case set 1

Figure 4.14 shows the relations between travel time and cumulative braking energy. Table 4.6 shows the existing conditions at the begin-braking points for case 1 to case 4. In Table 4.6, the summation of train kinetic and potential energy for cases with deeper alignments is low. This is because cases with deeper alignments operate in shorter travel time and acquire less kinetic

energy from traction motors. Moreover, due to the high operating speed for trains on dipped alignment, they waste more kinetic energy in air resistance and require less breaking energy to stop.

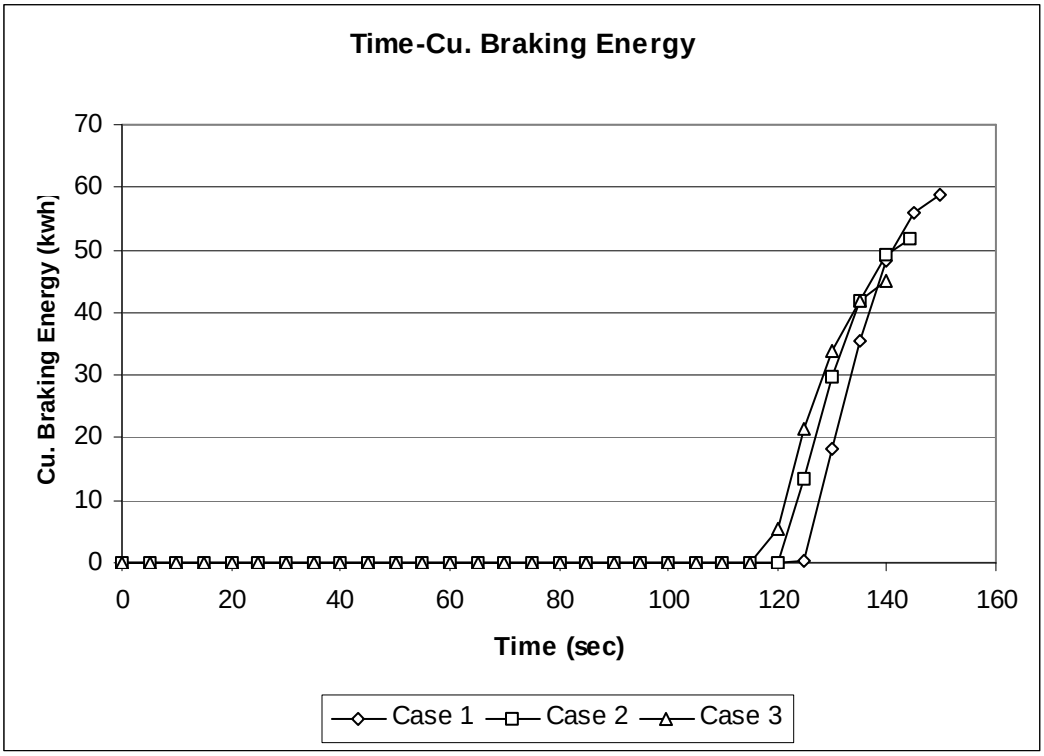

Figure 4.14 Time-Cumulative braking energy relations for baseline case set 1

Table 4.6 Existing conditions at begin-braking points for selected baseline cases

	Begin-Braking Point (ft)	Travel Time (sec)	Elevation (ft)	Speed (ft/s)	Kinetic plus Potential Energy (lb-ft^2/s^2)
Case 1	10966	124.9	0	118.90	7069*m_t^*
Case 2	11176	121.3	-5.8	112.47	6139* m_t^*
Case 3	11348	118.5	-8.1	105.45	5297* m_t^*
Case 4	11161	118.6	-23.4	113.69	5707* m_t^*

Note: m_t^* = Train mass in pounds

The energy conservation law can be used to explain why the savings for cases with the same parabolic curve length S are roughly proportional to the maximum depth δ. By the energy conservation law, if the air friction is negligible, all released potential energy from vertical drop should transform to kinetic energy. The energy conservation equation is listed below

$$m_t gh = \frac{1}{2} m_t (V_0 + \Delta V)^2 - \frac{1}{2} m_t (V_0)^2 \quad \text{or} \quad \Delta V = \frac{-2V_0 + \sqrt{4V_0^{\,2} + 8gh}}{2} \qquad (4.1)$$

where ΔV is the speed increment caused by vertical drop

V_0 is initial speed

m_t is train mass

g is acceleration due to gravity

h is vertical drop

For the above equation, if the initial speed V_0 is much greater than zero, the speed increment ΔV will be approximately proportional to the vertical drop h. The alignment equations in Table 3.1 show that the vertical drops h for cases with the same total curve length S are proportional to the coefficient δ (maximum depth). Therefore, the speed increment ΔV for dipped alignment is also approximately proportional to the maximum depth δ and the reduction of total travel time will be also roughly proportional to the maximum depth δ (Figure 4.9). Moreover, because the tractive energy consumption strongly depends on travel time and the braking energy consumption strongly depends on tractive energy consumption, the resulting tractive energy consumption and braking energy consumption should also be approximately proportional to the maximum depth δ.

4.4.2 Performance Profile Comparison for Case Set 2

The second set of baseline cases contains one level track and two dipped track alignments with the same maximum depth δ (60ft) but different total curve length S (12000ft; 6000ft). In this set of baseline cases, the savings for travel time, tractive energy and braking energy are listed in Table 4.7. For the two dipped alignments, the saving rates increase as the total curve length S decreases.

Table 4.7 Travel time, tractive energy and braking energy for baseline case set 2

	Case1 (S=12000; δ=0)		Case 2 (S=12000; δ=60)		Case 4 (S=6000; δ=60)	
	Profile	Saving*	Profile	Saving*	Profile	Saving*
Travel Time (sec)	149.45	0%	143.83	-3.76%	141.19	-5.53%
Tractive E. (kwh)	106.48	0%	103.47	-2.82%	101.87	-4.33%
Braking E. (kwh)	58.82	0%	51.71	-12.10%	48.62	-17.35%

Saving* is the difference in percentage compared to results of level track

Figures 4.15 and 4.16 show the relations between train locations and their elevation or gradient for baseline case set 2. In this set, trains in case 2 dives/rises to/from the maximum depth (60 ft) with a smaller gradient change (within ± 2%) and over a longer distance (250~6250 ft; 6250~12250 ft) while trains in case 4 dives/rises to/from the maximum depth (60 ft) with a greater gradient change (within ± 4 %) and over a shorter distance (250~3250 ft; 9250~12250 ft).

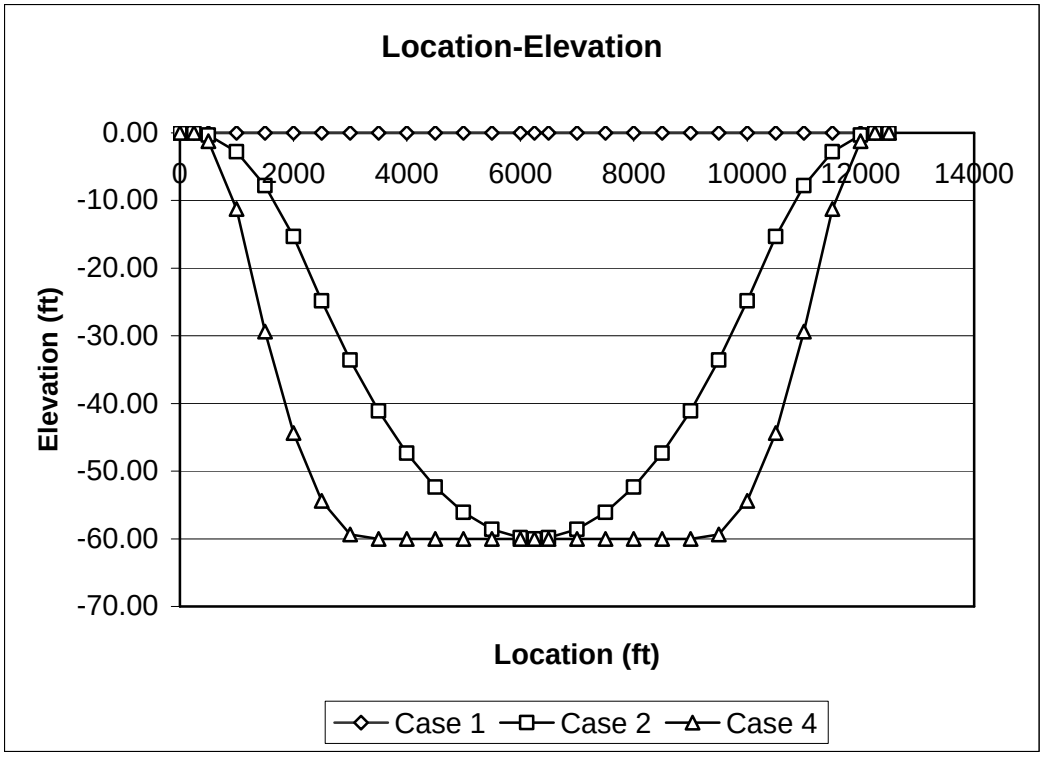

Figure 4.15 Location-Elevation relations for baseline case set 2

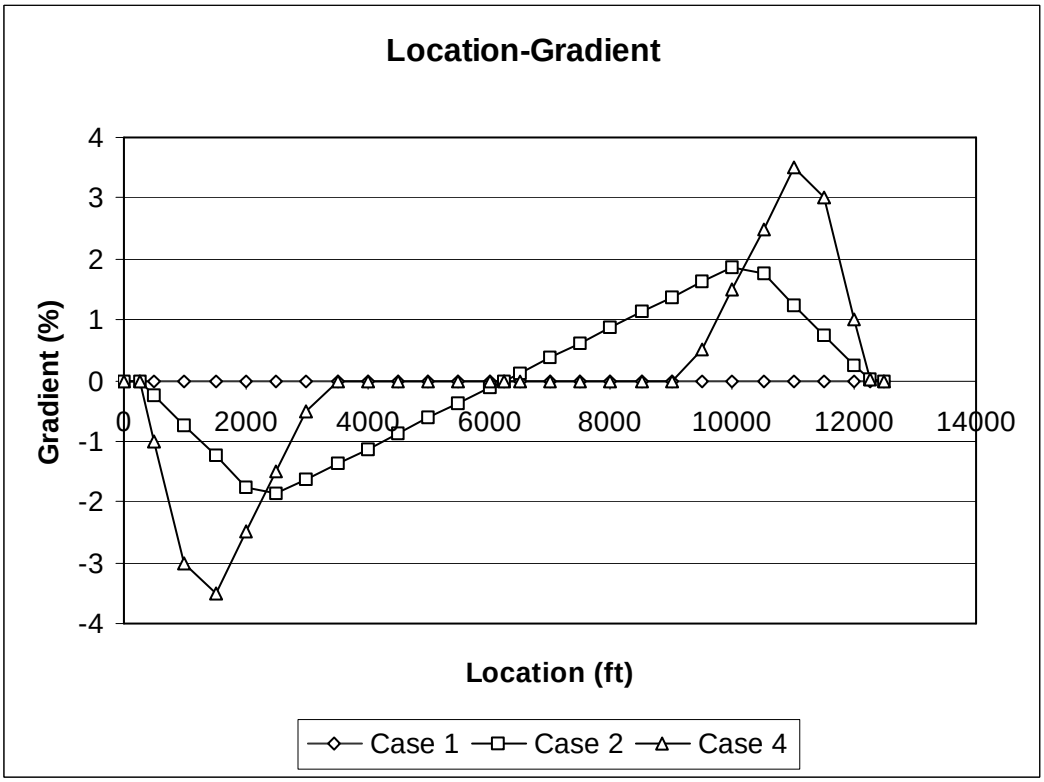

Figure 4.16 Location-Gradient relations for baseline case set 2

Figure 4.17 shows the location-resistance relations for baseline case set 2. The train resistances on dipped vertical track alignments are influenced by the track gradient.

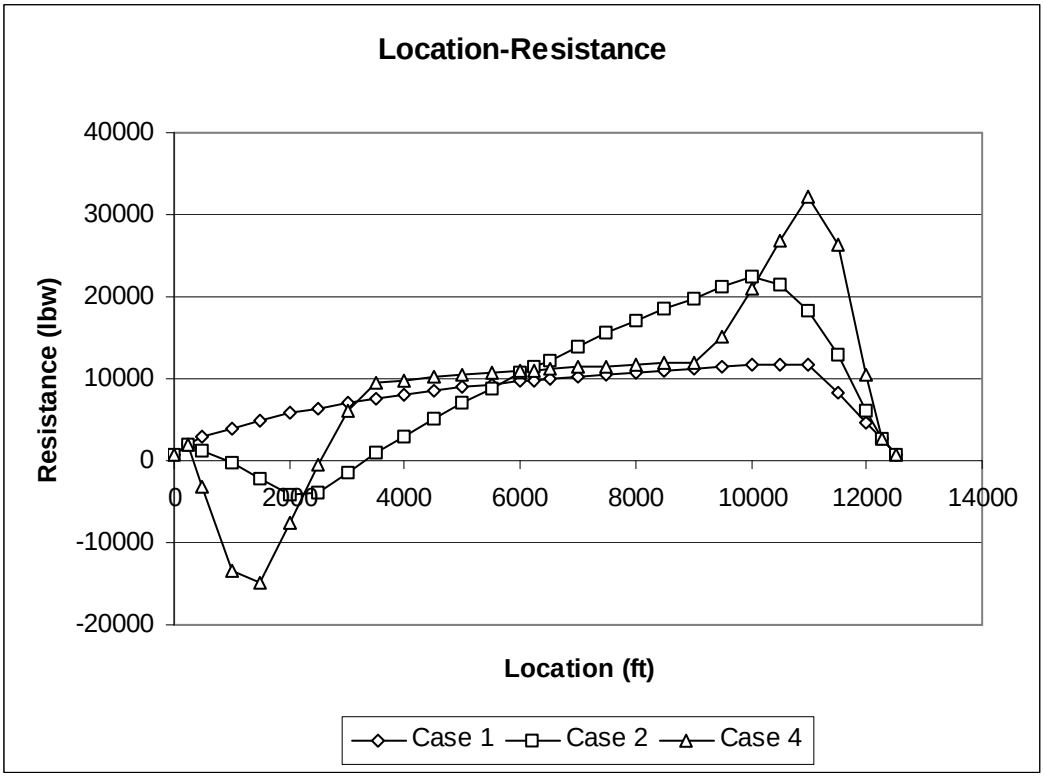

Figure 4.17 Location-Resistance relations for baseline case set 2

Figure 4.18 shows the location-acceleration relation. Trains in case 1 on level track accelerate smoothly until starting brake. Trains in case 2 on long curve accelerate with slightly faster than trains in case 1 for the first half (descending) section and slightly slower than trains in case 1 for the second half (climbing) section. Trains in case 4 accelerate with high rate within its descending section (0~3250 ft) and operates in high speed without deceleration within the level section (3250~9250 ft).

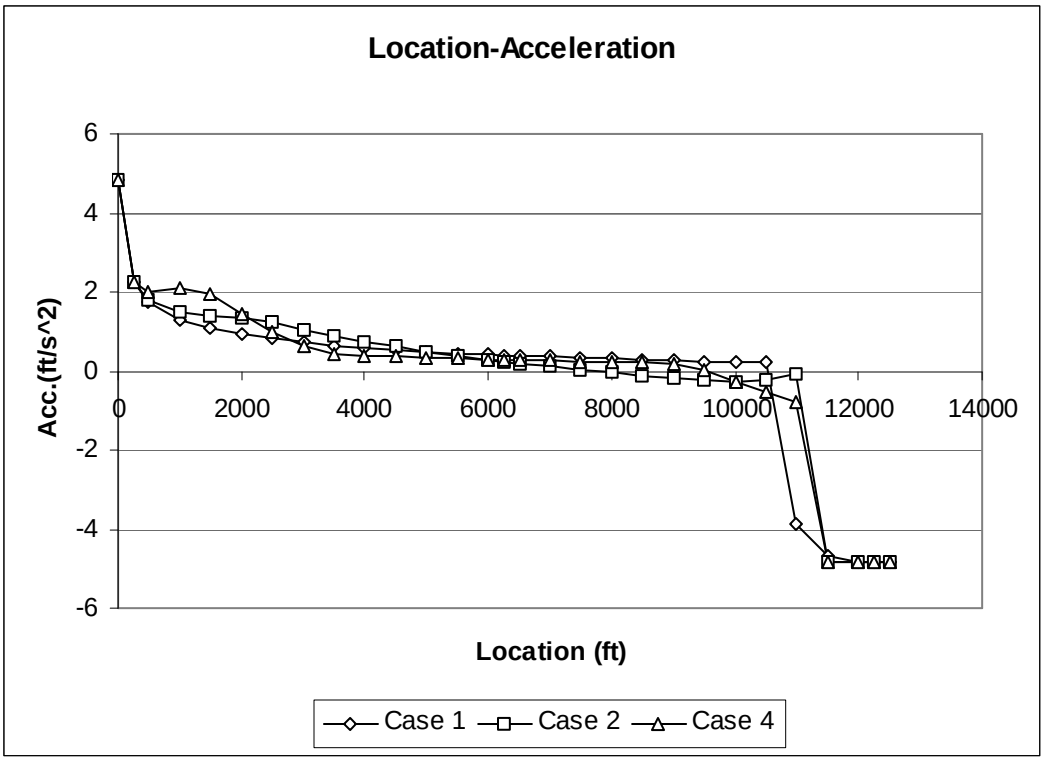

Figure 4.18 Location-Acceleration relations for baseline case set 2

Figures 4.19 and 4.20 show location-speed and location-time diagrams. In general, trains operating on steeper vertical alignments gather more advantages in accelerating to high speed early and have less travel time between stations.

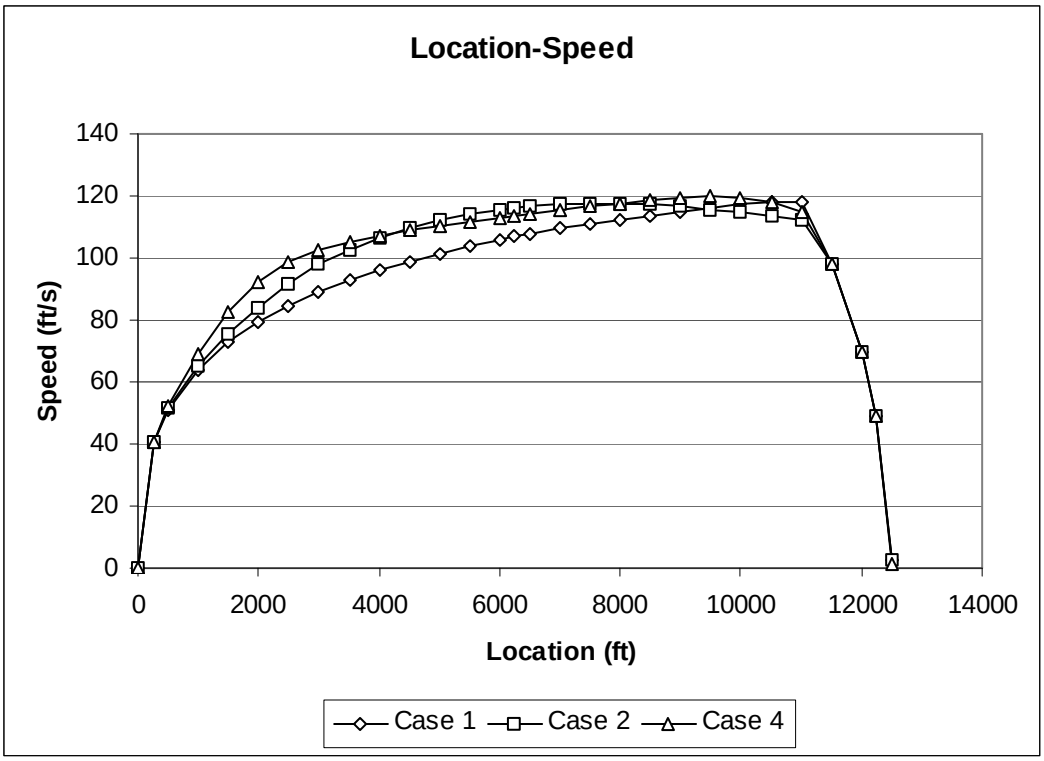

Figure 4.19 Location-Speed relations for baseline case set 2

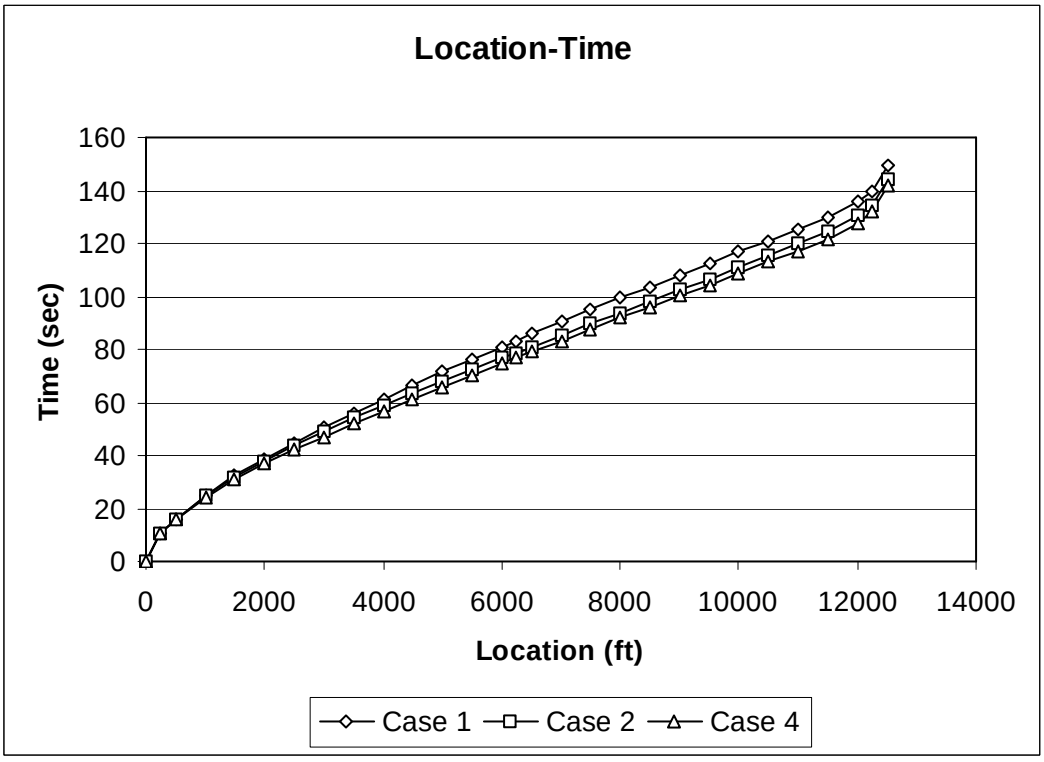

Figure 4.20 Location-Time relations for baseline case set 2

Figures 4.21 and 4.22 show time-acceleration and time-speed relations. From the two diagrams, trains in case 4 accelerate at a higher rate at the beginning and begins decelerating earlier than trains in case 2.

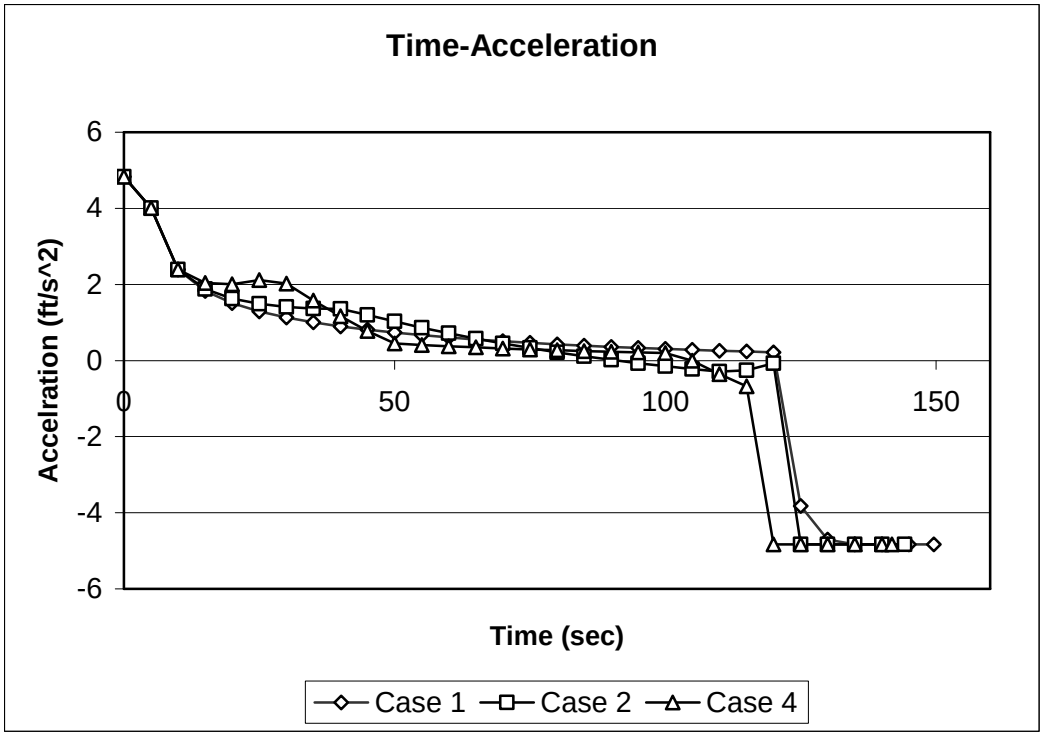

Figure 4.21 Time-Acceleration relations for baseline case set 2

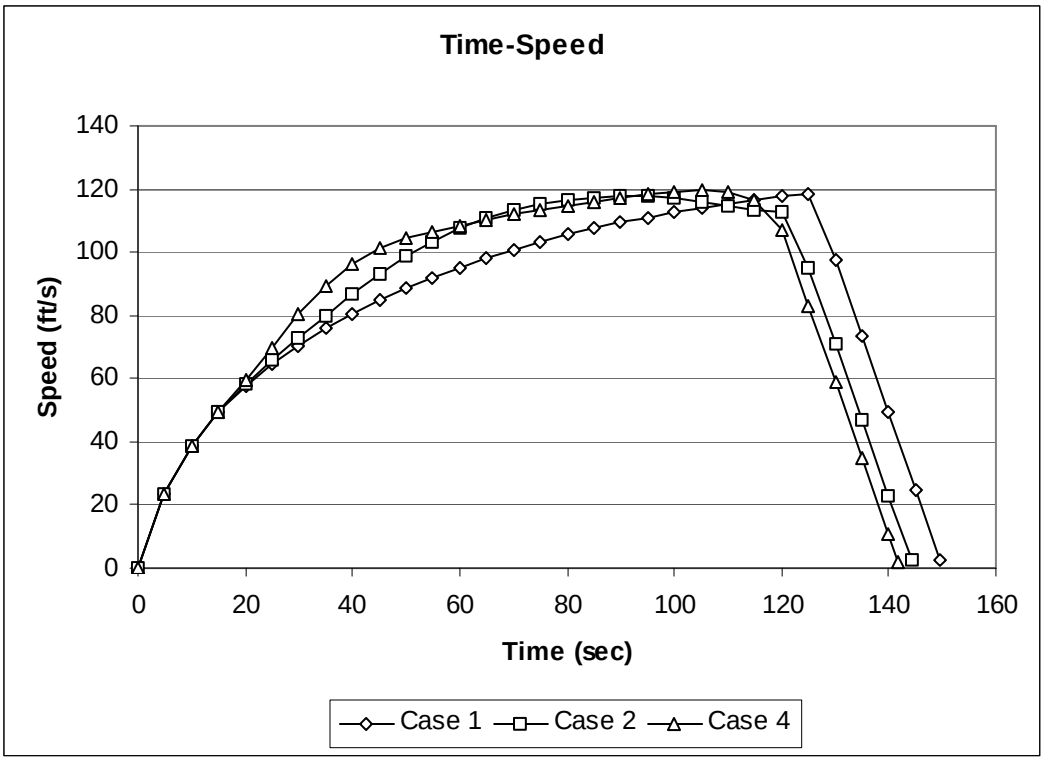

Figure 4.22 Time-Speed relations for baseline case set 2

Figure 4.23 shows the time-cumulative tractive energy relations. As mentioned earlier, trains reaching their begin-raking points faster consume less tractive energy. In Table 4.6, trains in case 4 are the earliest reaching begin-braking point and consume the least tractive energy.

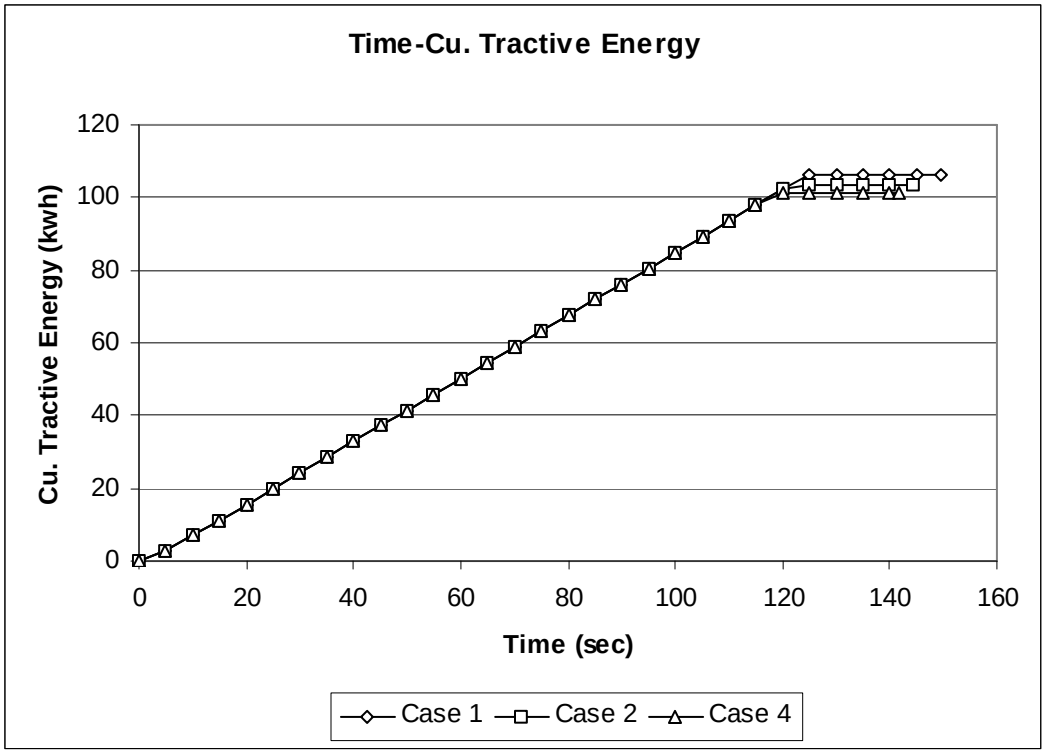

Figure 4.23 Time-Cumulative tractive energy relations for baseline case set 2

Figure 4.24 shows the relations between travel time and cumulative braking energy. In the results of Table 4.6, trains in case 4 need less braking energy than trains in case 2 because at the begin-braking point the initial speeds for the two dipped alignments are almost the same but elevation for trains in case 4 are lower than trains in case 2.

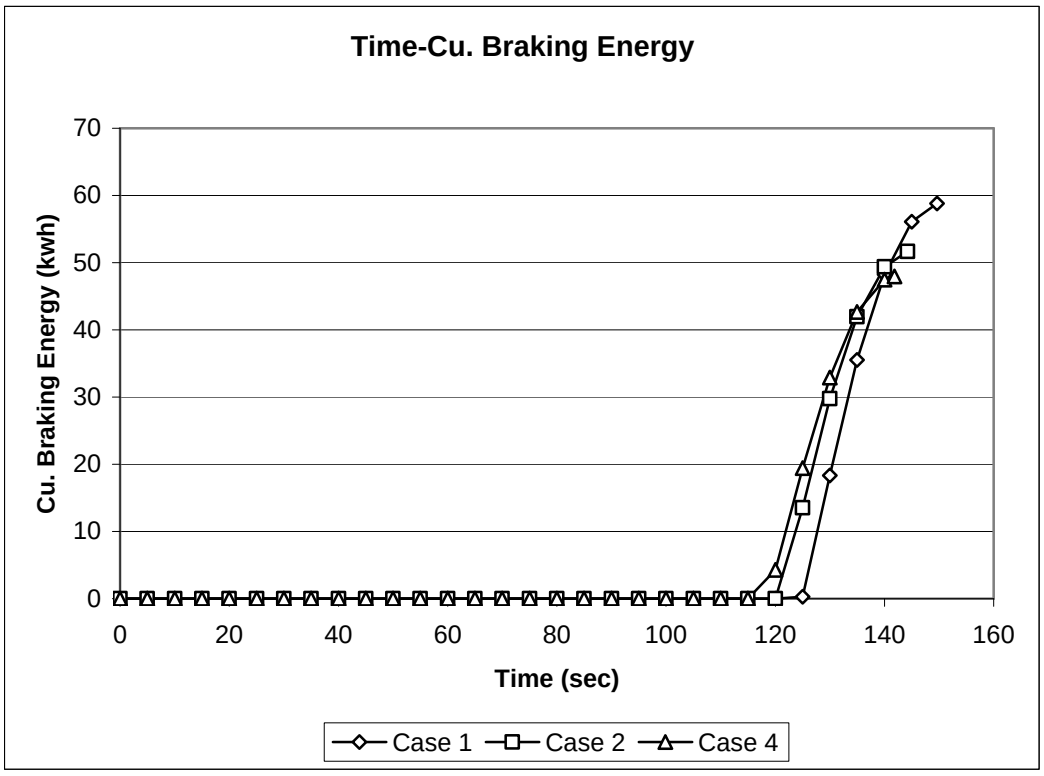

Figure 4.24 Time-Cumulative braking energy relations for baseline case set 2

In conclusion, for simulation cases with the same maximum depth δ but different total curve length S, trains in cases with shorter S have advantages in accelerating to high speed early to reduce total travel time and tractive energy consumption. Moreover, because of the late rise in alignment for cases with short total curve length S, the elevations for trains at begin-braking point are lower and result in lower braking energy consumption.

4.5 Sensitivity Analysis

The purpose of this section is to analyze the sensitivity of results to parameter changes listed in Table 4.8. For each instance of sensitivity analysis, the value of a selected parameter will be replaced by the new value in Table 4.8 while other operating parameters will remain at their baseline values.

Table 4.8 Parameters for sensitivity analysis

	Baseline assumptions	Sensitivity analysis	Unit
Acceleration constraint	4.827	3.218	ft/s^2
Power per car	520	400	KW
Speed constraint	No constraint	75	MPH
Dist. begin coasting	No coasting	4000	Feet
Air resis. coeff.	3X as Davis Eq.	As Davis Eq.	-
Car weight	50	40	Ton
Station spacing	12500	8500	Feet

4.5.1 Sensitivity Analysis Results

In this sensitivity analysis, four vertical track alignment designs are investigated as in Table 4.9. The simulation results for sensitivity analysis are shown in Tables 4.10-4.12.

Table 4.9 Vertical track alignments for sensitivity analysis

	Total curve length S (ft)	δ/S ratio	Level bottom (ft)
Alignment I	-	0	-
Alignment II	L_{ss}-L_{pl}	0.5%	0
Alignment III	L_{ss}-L_{pl}	1%	0
Alignment IV	½ (L_{ss}-L_{pl})	1%	½ (L_{ss}-L_{pl})

L_{ss}: Station spacing L_{pl}: Length of platform

Table 4.10 Sensitivity analysis for travel time

Travel time (Sec)	Alignment I		Alignment II		Alignment III		Alignment IV	
	Profile	Saving	Profile	Saving	Profile	Saving	Profile	Saving
Baseline assumptions	149.60	0	144.22	-5.38 -3.60%	140.04	-9.56 -6.39%	141.83	-7.76 -5.19%
Acc. Const: 3.218 ft/s^2	157.91	0	152.34	-5.57 -3.53%	147.34	-10.56 -6.69%	149.90	-8.01 -5.07%
Power per car: 400 KW	160.31	0	154.18	-6.13 -3.83%	148.92	-11.39 -7.10%	150.90	-9.41 -5.87%
Speed const: 75 MPH	151.27	0	147.20	-4.07 -2.69%	147.24	-4.02 -2.66%	145.03	-6.23 -4.12%
Coasting Dist: 4000 feet	151.92	0	147.19	-4.73 -3.11%	143.86	-8.06 -5.31%	144.28	-7.64 -5.03%
Air res. coeff: As Davis Eq.	143.47	0	137.37	-6.10 -4.25%	132.74	-10.73 -7.48%	134.91	-8.56 -5.97%
Car weight: 40 ton	143.46	0	139.17	-4.29 -2.99%	135.59	-7.87 -5.49%	137.30	-6.16 -4.30%
Station spacing 8500 feet	114.84	0	111.19	-3.65 -3.18%	107.89	-6.95 -6.05%	109.34	-5.50 -4.79%

*Saving is the difference in value or in percentage compared with case with the same assumptions but operating on level track (Alignment I)

Table 4.11 Sensitivity analysis for tractive energy consumption

Tractive Energy (KWH)	Alignment I		Alignment II		Alignment III		Alignment IV	
	Profile	Saving	Profile	Saving	Profile	Saving	Profile	Saving
Baseline assumptions	106.48	-	103.34	-3.14 -2.95%	100.91	-5.57 -5.23%	101.02	-5.46 -5.13%
Acc. Const: 3.218 ft/s^2	101.72	-	97.99	-3.74 -3.67%	95.43	-6.29 -6.18%	94.49	-7.24 -7.11%
Power per car: 400 KW	91.31	-	87.97	-3.34 -3.65%	85.59	-5.71 -6.26%	85.95	-5.36 -5.87%
Speed const: 75 MPH	97.01	-	96.12	-0.89 -0.91%	88.34	-8.66 -8.93%	91.13	-5.88 -6.06%
Coasting Dist: 4000 feet	88.14	-	83.15	-4.99 -5.66%	79.00	-9.13 -10.36%	81.55	-6.59 -7.47%
Air res. coeff: As Davis Eq.	96.88	-	93.11	-3.77 -3.89%	90.00	-6.88 -7.10%	90.73	-6.15 -6.35%
Car weight: 40 ton	100.01	-	97.84	-2.16 -2.16%	96.15	-3.85 -3.85%	95.86	-4.15 -4.15%
Station spacing 8500 feet	78.21	-	75.75	-2.45 -3.14%	73.67	-4.53 -5.80%	73.84	-4.36 -5.58%

*Saving is the difference in value or in percentage compared with case with the same assumptions but operating on level track (Alignment I)

Table 4.12 Sensitivity analysis for braking energy consumption

Braking Energy (KWH)	Alignment I		Alignment II		Alignment III		Alignment IV	
	Profile	Saving	Profile	Saving	Profile	Saving	Profile	Saving
Baseline assumptions	58.83	-	51.65	-7.18 -12.21%	44.95	-13.88 -23.59%	47.95	-10.88 -18.50%
Acc. Const: 3.218 ft/s^2	56.05	-	47.99	-8.06 -14.38%	40.84	-15.21 -27.14%	43.32	-12.73 -22.71%
Power per car: 400 KW	50.12	-	42.96	-7.16 -14.28%	36.36	-13.76 -27.46%	39.52	-10.60 -21.15%
Speed const: 75 MPH	51.00	-	47.64	-3.36 -6.60%	40.23	-10.77 -21.12%	41.56	-9.44 -18.51%
Coasting Dist: 4000 feet	42.58	-	33.86	-8.72 -20.47%	25.75	-16.83 -39.53%	30.82	-11.76 -27.61%
Air res. coeff: As Davis Eq.	75.62	-	69.88	-5.74 -7.59%	64.77	-10.85 -14.34%	66.94	-8.68 -11.48%
Car weight: 40 ton	48.93	-	43.10	-5.84 -11.93%	37.57	-11.36 -23.22%	39.86	-9.07 -18.54%
Station spacing 8500 feet	51.19	-	46.59	-4.59 -8.98%	42.23	-8.95 -17.49%	44.00	-7.19 -14.05%

*Saving is the difference in value or in percentage compared with case with the same assumptions but operating on level track (Alignment I)

4.5.2 Analysis of Sensitivity Results

Figures 4.25-4.28 show the speed-location relations for sensitivity analysis on various vertical alignments. Table 4.13 shows the existing conditions at the begin-braking points for sensitivity analysis. The four speed diagrams and the begin-braking condition table show changes in travel time, tractive energy consumption and braking energy consumption in the sensitivity analysis.

Effect of Maximum Allowable Acceleration

While operating with a low acceleration constraint, the saving for travel time and braking energy increases slightly. The change in maximum allowable acceleration rate result in only a small change because the acceleration constraint only effects small fraction of time in total simulation period (only for the first and last few seconds of acceleration and deceleration) (Figures 4.25-4.28). Because of the long braking distances due to the low deceleration rate, the begin-braking points for dipped alignments will be located lower and result more braking energy saving from potential energy.

Effects of Power and Vehicle Weight

Greater percentage savings are observed for low power vehicles on dipped alignments. Moreover, when vehicle weight decreases, the saving on dipped alignments decreases.

In theory, the speed increment ΔV from released potential energy is

$$\Delta V = \frac{-2V_0 + \sqrt{4V_0^2 + 8gh}}{2} \tag{4.1}$$

If the power/weight ratio increases, the train speed on level track will increases too. Thus, because of the higher initial speeds V_0 for trains on level alignment, the speed increments ΔV from potential energy while using dipped alignment will be lower (Figures 4.25-4.28) and result in fewer saving in travel time and tractive energy consumption.

Effect of Speed Constraint

With a low speed limit, the savings in travel time, tractive energy consumption and braking energy consumption are lower than without speed limit and are no longer proportional to the maximum depth δ for cases with the same total curve length S. Trains reaching the speed limit within a descending section cannot transform potential energy into kinetic energy by accelerating to higher speeds.

Effect of Train Coasting

Coasting can increase the percentage savings in tractive energy and braking energy. In Tables 4.10-4.12, when coasting, the percentage of saving in travel time drops slightly but savings in tractive energy and braking energy consumption are almost doubled. Coasting does not significantly increase travel time is because the non-power operating only results in small speed drop for the last few seconds (Figures 4.25-4.28). Trains cut off their traction power early and save more tractive energy by using coasting. Table 4.13 shows that compared with coasting on level track, trains coasting on a dipped alignment decelerate more before starting to brake and require less braking energy to stop.

Effect of Air Friction

An air resistance coefficient used for trains operating outside tunnels is applied in this sensitivity analysis. Low air friction increases the travel time and the tractive energy consumption benefits from using dipped alignments. Therefore, in this sensitivity analysis, low air friction amplifies (Figures 4.25-4.28) the train speed increments on dipped alignments and results more saving in travel time. Moreover, cutting off traction motors early also reduces the tractive energy consumption. However, the low air friction results in lower speed reductions during braking and less advantage in helping to stop trains.

Effect of Station Spacing

The percentage savings for travel time and tractive energy consumption are not significant changed by applying different station spacings. However, for cases with dipped alignments and long station spacing, the initial speed at begin-braking point should be high. Thus, trains on long and dipped alignment waste more kinetic energy in air friction during braking and require less braking energy consumption.

Table 4.13 Begin-braking information for sensitivity analysis

	Changing Variables	Begin-Braking Point (ft)	Travel Time (sec)	Elev. (ft)	Speed (ft/s)	Kinetic plus Potential Energy (lb-ft^2/s^2)
Alignment I	Baseline assum.	10966	124.9	0	118.90	$7069*m_t$
	Max. acc. :0.1g	10346	122.0	0	117.74	$6932*m_t$
	Pow/car:400kw	11246	138.5	0	109.07	$5948*m_t$
	Spd cons:75mph	11221	128.7	0	110.00	$6050*m_t$
	Coasting:4000 ft	11462	131.5	0	99.93	$4993*m_t$
	1x air resistance	10357	113.8	0	132.62	$8794*m_t$
	Weig/car:40 ton	10863	117.9	0	122.74	$7533*m_t$
	Stat Spa:8500 ft	7216	92.3	0	110.22	$6074*m_t$
Alignment II	Baseline assum.	11176	121.3	-5.8	112.47	$6139*m_t$
	Max. acc. :0.1g	10510	117.6	-15.1	113.15	$5915*m_t$
	Pow/car:400kw	11432	133.5	-3.3	101.51	$5044*m_t$
	Spd cons:75mph	11299	125.5	-4.5	107.49	$5631*m_t$
	Coasting:4000 ft	11673	129.0	-1.7	89.31	$3935*m_t$
	1x air resistance	10549	109.5	-14.5	130.78	$8087*m_t$
	Weig/car:40 ton	11084	115.5	-6.8	116.28	$6542*m_t$
	Stat Spa:8500 ft	7316	89.5	-6.5	106.87	$5500*m_t$
Alignment III	Baseline assum.	11348	118.5	-8.1	105.45	$5297*m_t$
	Max. acc. :0.1g	10708	114.7	-23.8	107.38	$5001*m_t$
	Pow/car:400kw	11593	130.0	-4.3	93.58	$4239*m_t$
	Spd cons:75mph	11540	127.9	-5.0	96.30	$4474*m_t$
	Coasting:4000 ft	11876	128.1	-1.4	77.60	$2966*m_t$
	1x air resistance	10714	105.9	-23.6	128.20	$7458*m_t$
	Weig/car:40 ton	11266	113.5	-9.7	109.13	$5644*m_t$
	Stat Spa:8500 ft	7398	87.1	-10.9	103.15	$4969*m_t$
Alignment IV	Baseline assum.	11161	118.6	-23.5	113.69	$5707*m_t$
	Max. acc. :0.1g	10319	113.6	-48.6	118.47	$5455*m_t$
	Pow/car:400kw	11455	130.5	-12.6	100.43	$4637*m_t$
	Spd cons:75mph	11387	124.0	-14.9	103.66	$4893*m_t$
	Coasting:4000 ft	11722	126.7	-5.6	86.64	$3574*m_t$
	1x air resistance	10509	106.7	-44.1	135.28	$7730*m_t$
	Weig/car:40 ton	11058	113.2	-27.3	117.96	$6078*m_t$
	Stat Spa:8500 ft	7253	87.3	-24.9	109.72	$5218*m_t$

Note: m_t = Train mass in pounds

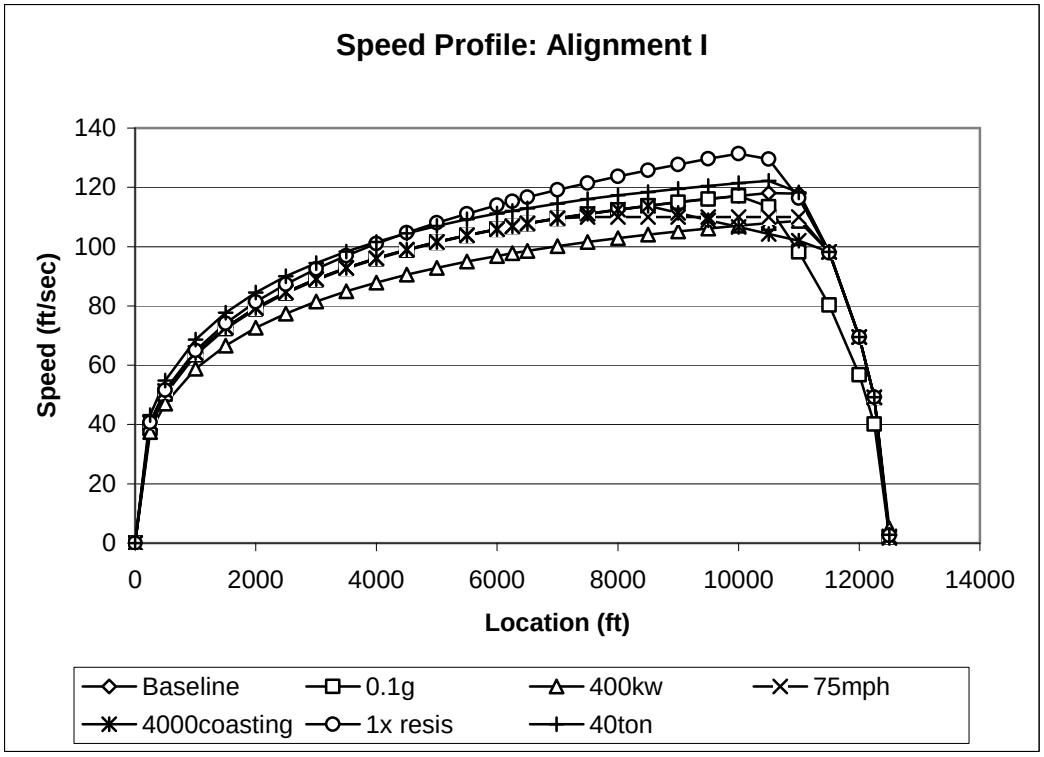

Figure 4.25 Sensitivities of train speeds to parameter changes for alignment I

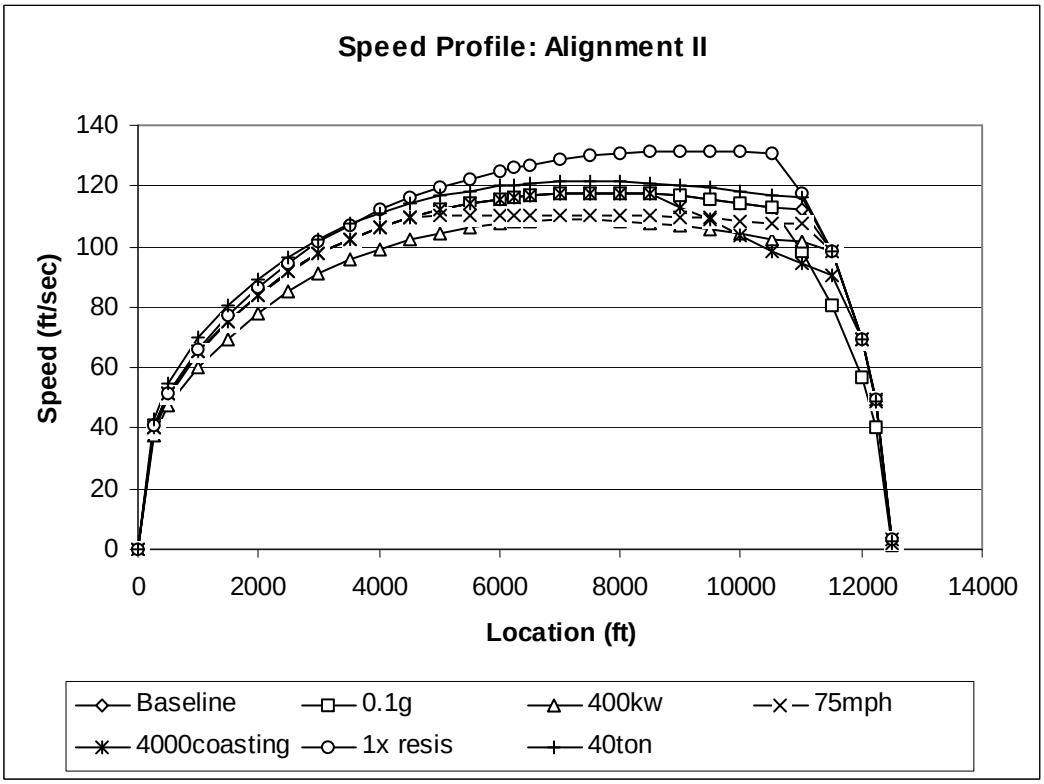

Figure 4.26 Sensitivities of train speeds to parameter changes for alignment II

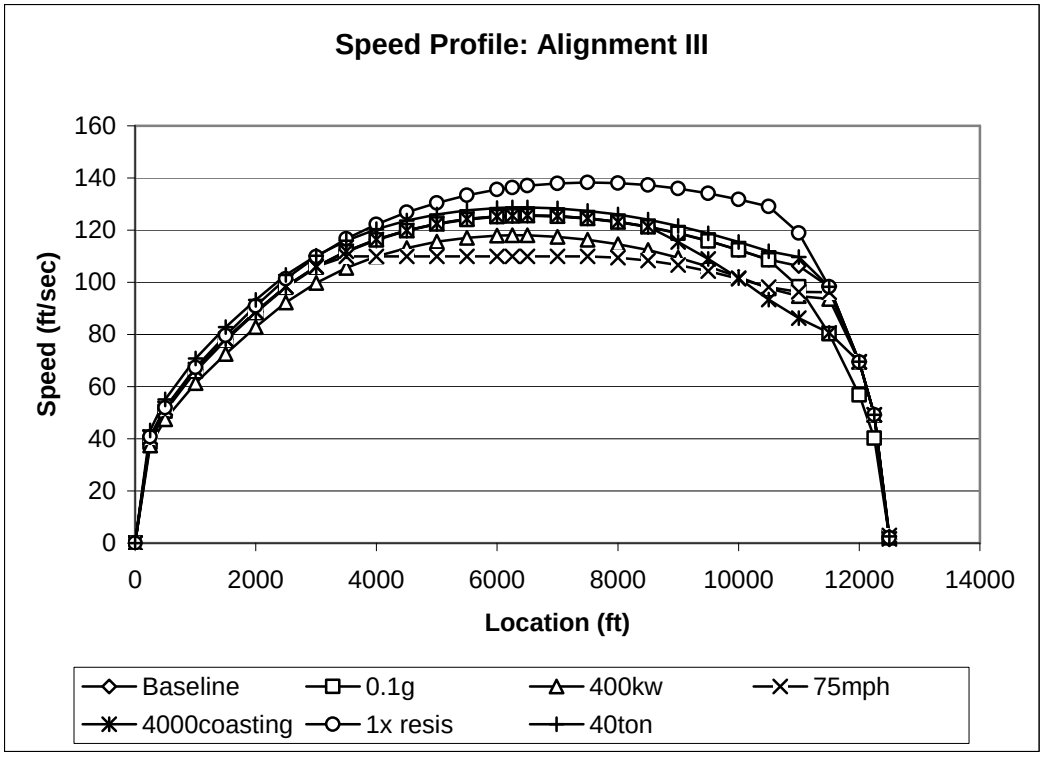

Figure 4.27 Sensitivities of train speeds to parameter changes for alignment III

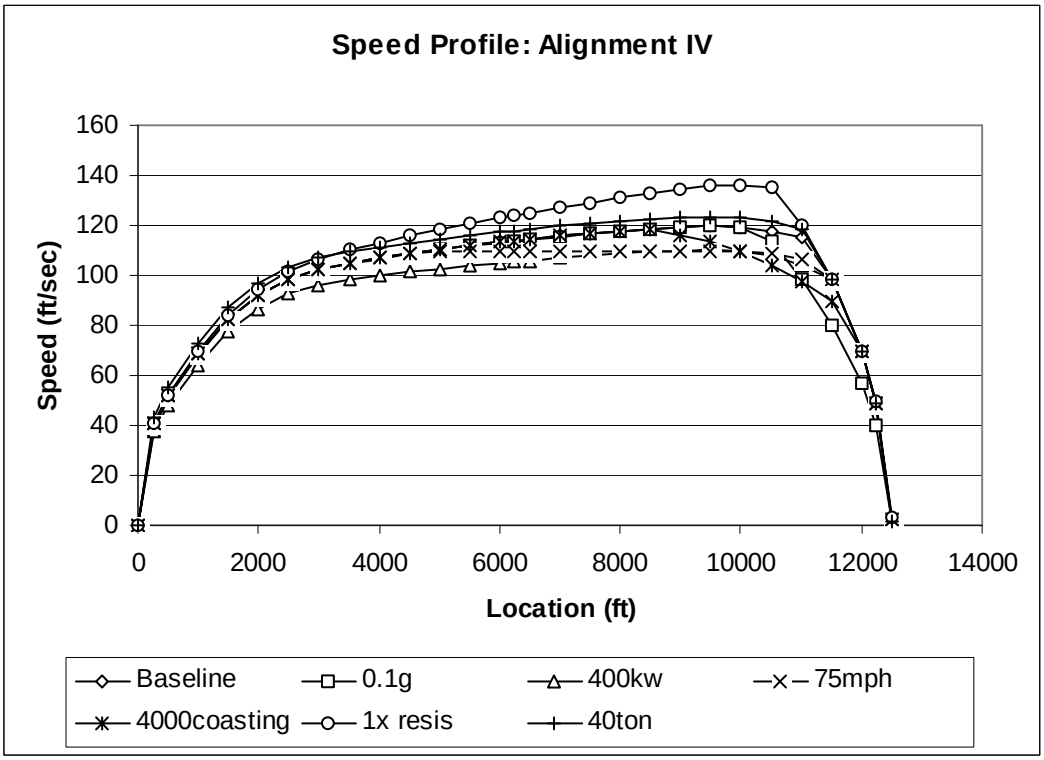

Figure 4.28 Sensitivities of train speeds to parameter changes for alignment IV

Chapter 5. Optimization of Simulation Results

5.1 Optimization Methods

The total cost function C_t in this study is only for a one-directional operation between stations. As mentioned in Section 3.6, total cost C_t for a one-directional operation between stations includes user-in-vehicle cost, vehicle capital expenses (vehicle depreciation), tractive energy expenses, braking wear expenses and construction cost.

Because we assume the construction cost increments is not increased for dipped alignments. It can be simplified as zero for any alignment design in these total cost evaluations and comparisons. However, if construction cost was depth-related, the benefits of using dipped alignment in rail transit system could, of course, decrease. Table 5.1 shows the baseline values used in the total cost function for the following analysis.

Table 5.1 Baseline values used in total cost function

Variable	Definition	Value	Units
n_p	Average passengers per car	50	Psg/car
v_{user}	Value of user time	5	$/psg-hr
$v_{vehicle}$	Vehicle depreciation per revenue hour	50	$/car-hr
$C_{construction}$	Average construction cost for an one-directional operation between stations	0	$/one-directional operation
$v_{tractive}$	Unit tractive energy cost	0.15	$/kwh
$v_{braking}$	Unit braking energy cost	0.1	$/kwh

The baseline case and sensitivity study in Chapter 4 show that the simulation results are smooth and continuous with respect to all simulation parameters. Therefore, Golden Section Search in one-dimensional optimizations and Powell's Method in multi-dimensional optimization can be used with the deterministic simulator to minimize the total cost function.

5.2 Joint Optimization of Total Cost

Three station spacings (16,500 ft; 12500 ft; 8500 ft) are selected in the joint optimization studies. For all jointly optimizing problems, excepting changing variables, all other variables will use baseline assumed values as mentioned in Section 4.1.

Table 5.2 shows jointly optimized solutions for the following changing variables: alignment coefficients S and δ (for dipped alignment only), speed constraint V_{cruise} and coasting distance $d_{coasting}$. The optimizations demonstrate the following points:

1. The optimized speed limits are equal to their maximum speeds. Therefore, unconstrained speeds are the optimized solutions for speed constraints.
2. Without a speed constraint, the percentage savings for using optimized dipped alignments are about 6.7%
3. Without a speed constraint, the optimized alignment depths are about 0.75% of station spacings.
4. Without a speed constraint, the δ/S ratio for optimized alignment is about 1% (the maximum allowable δ/S value)

Table 5.2 Jointly optimized alignments, speed constraints and coasting distance

		Station Spacing: 8,500 ft		Station Spacing: 12,500 ft		Station Spacing: 16,500 ft	
Alignment		Level	Dipped	Level	Dipped	Level	Dipped
Optimized	S (ft)	-	6595	-	10241	-	11915
	δ (ft)	0.0	62.3	0.0	101.1	0.0	117.0
	$V_{cruise\ (mph)}$	64.2	73.4	73.7	83.3	79.1	87.1
	$d_{coasting}$ (ft)	3777	3842	4954	4759	5951	4498
Performance measures	V_{max} (mph)	64.2	73.4	73.7	83.3	79.1	87.0
	L_{vmax} (ft)	3697	3983	6592	6724	9481	10487
	T (sec)	120.34	113.07	155.03	145.90	188.72	175.49
	E_t (kwh)	52.26	50.23	77.65	73.33	101.14	102.83
	E_b (kwh)	28.92	22.53	34.84	22.23	36.96	25.04
	C_t ($)	**70.90**	**66.32**	**92.65**	**86.17**	**113.23**	**105.67**
	C_t Saving ($)	**-**	**-4.58**	**-**	**-6.47**	**-**	**-7.55**
	C_t Saving (%)	**-**	**-6.46**	**-**	**-6.99**	**-**	**-6.67**

Tables 5.3 and 5.4 show the Jointly optimized solutions for alignment coefficients S and δ (for dipped alignment only), and coasting distance $d_{coasting}$ while speed constraints are pre-specified (75 mph & 55 mph). Tables 5.3 and 5.4 show the following points for optimized solutions with low speed constraints:

1. For optimized alignments with a low speed constraint, trains accelerate to the speed constraint approximately at the point (L_{vmax}) where the descending curves are finished ($L_{pl}/2 + S/2$).
2. Optimized parabolic curve designs for cases with the same speed constraint but different station spacings are approximately equivalent to each other. Moreover, the optimized total cost savings are approximately equal for cases with the same speed constraints but different station spacings (Tables 5.3 and 5.4 show $5.4 total cost savings for a one-directional operation with a 75mph speed constraint and $2.1 with a 55mph speed constraint).
3. The optimized total cost savings decreases as the speed limit decreases.
4. The optimized δ/S ratios are also approximately equal to 1.0 (the maximum allowable δ/S value) for operating with speed constraints.

Table 5.3 Jointly optimized alignments and coasting distance with a 75mph speed constraint

		Station Spacing: 8,500 ft		Station Spacing: 12,500 ft		Station Spacing: 16,500 ft	
Alignment		Level	Dipped	Level	Dipped	Level	Dipped
Optimized	S (ft)	-	7459	-	7654	-	8453
	δ (ft)	0.0	72.0	0.0	74.5	0.0	81.6
	$d_{coasting}$ (ft)	4393	4223	5641	3687	5009	3402
Performance measures	V_{max} (mph)	66.0	75.0	74.4	75.0	75.0	75.0
	L_{vmax} (ft)	4106	3946	6858	3799	7146	3581
	T (sec)	120.37	113.78	155.95	149.01	190.75	185.07
	E_t (kwh)	52.31	48.28	75.38	69.48	98.28	89.62
	E_b (kwh)	28.92	20.72	33.23	22.32	35.96	23.26
	C_t ($)	**70.92**	**66.20**	**92.61**	**87.16**	**113.71**	**108.30**
	C_t Saving ($)	**-**	**-4.72**	**-**	**-5.45**	**-**	**-5.41**
	C_t Saving (%)	**-**	**-6.65**	**-**	**-5.88**	**-**	**-4.76**

Table 5.4 Jointly optimized alignments and coasting distance with a 55mph speed constraint

		Station Spacing: 8,500 ft		Station Spacing: 12,500 ft		Station Spacing: 16,500 ft	
Alignment		Level	Dipped	Level	Dipped	Level	Dipped
Optimized	S (ft)	-	2906	-	3115	-	2954
	δ (ft)	0.0	26.9	0.0	29.5	0.0	27.4
	$d_{coasting}$ (ft)	2174	2610	2570	1783	2880	2440
Performance measures	V_{max} (mph)	55.0	55.0	55.0	55.0	55.0	55.0
	L_{vmax} (ft)	2119	1474	2119	1437	2119	1466
	T (sec)	127.60	127.42	177.73	176.15	227.68	226.41
	E_t (kwh)	44.43	36.28	54.21	48.72	64.21	58.31
	E_b (kwh)	24.33	16.17	23.42	17.49	22.70	16.43
	C_t ($)	**72.90**	**70.77**	**99.34**	**97.13**	**125.74**	**123.59**
	C_t Saving ($)	**-**	**-2.13**	**-**	**-2.21**	**-**	**-2.15**
	C_t Saving (%)	**-**	**-2.92**	**-**	**-2.22**	**-**	**-1.71**

5.3 Relations between Optimized Solutions and Alignment Depth

For some sites with poor geology (i.e. high ground water level), alignment designs are limited within certain depths. This section is focused on the relations between optimized total costs and specified alignment depths with various speed constraints. Simulation cases with three station spacings (8500 ft, 12500 ft, 16500 ft) and three speed constraints (unconstrained, 75 mph, 55 mph) with depth changes are optimized. The changing variables in this study are total curve length S and coasting distances $d_{coasting}$. Figures 5.1-5.3 show the optimized total cost vs. alignment depth relations. The following points are found in the optimization results:

1. Without speed constraints, the optimized total costs decrease as the alignment depth increases.
2. Without speed constraints, the marginal savings in total cost for unit increase in alignment depth of shallow tunnels are much higher than the marginal savings of deep alignments. Figures 5.1-5.3 show no significant total cost saving can be found by increasing tunnel depth beyond 60 ft.
3. For any constrained speed, an optimized alignment depth can be found. The optimized alignment depth decreases as the speed constraint decreases.

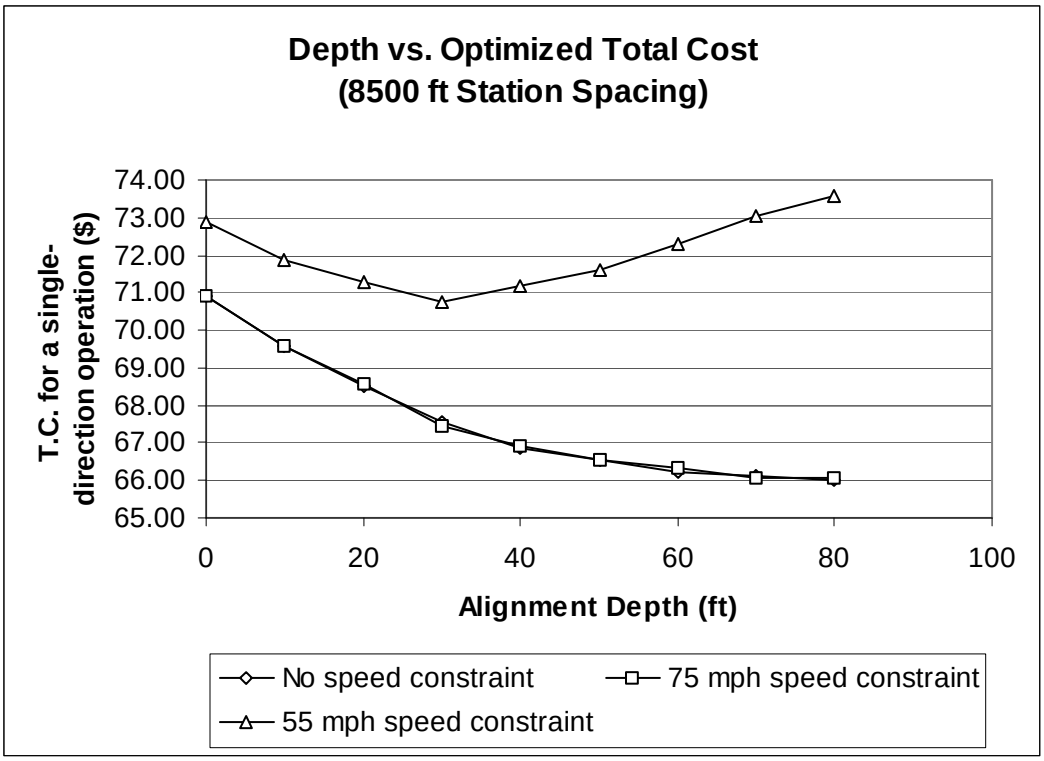

Figure 5.1 Depth-optimized total cost relations for 8500 ft station spacing

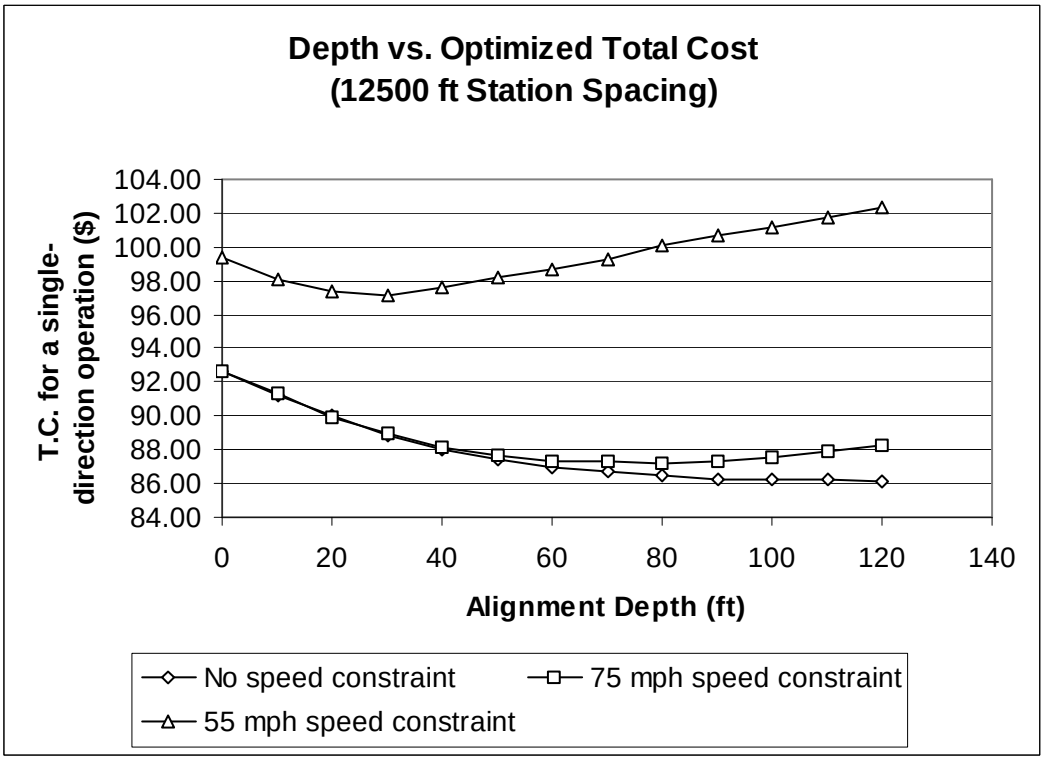

Figure 5.2 Depth-optimized total cost relations for 12500 ft station spacing

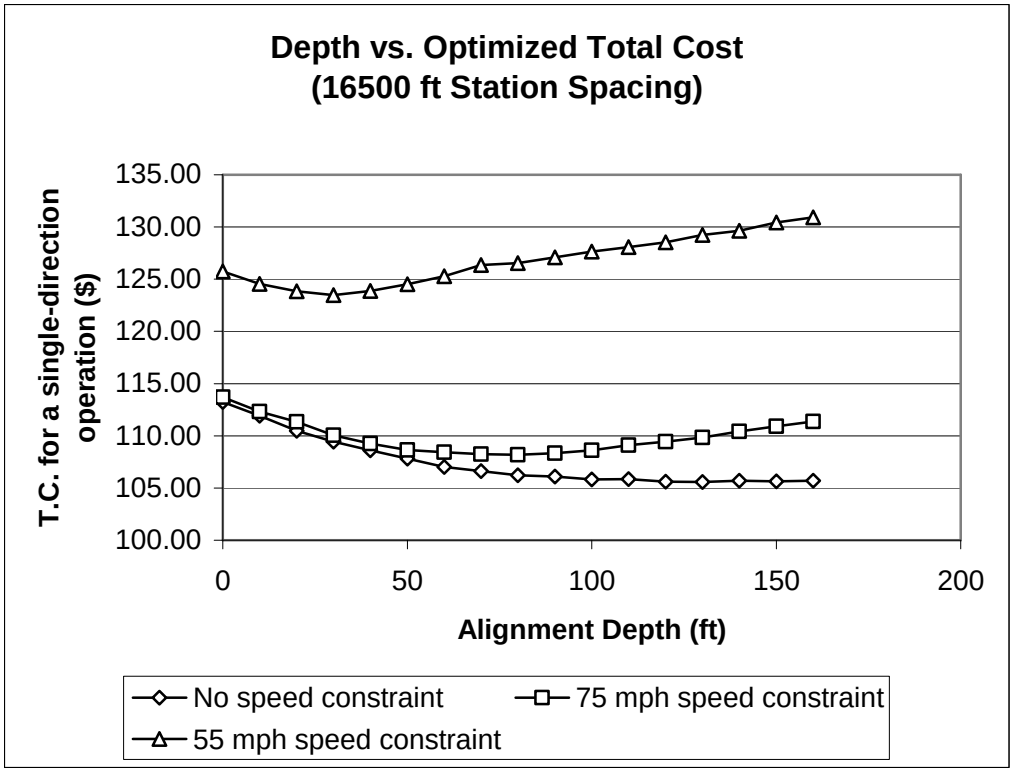

Figure 5.3 Depth-optimized total cost relations for 16500 ft station spacing

The three-dimensional relations between alignment depths, speed constraints and total costs for one-directional operations between 12,500 station spacing are shown in Figure 5.4. Combinations of 20 speed constraints and 25 alignment depths are optimized in this section. Figure 5.4 shows that optimized alignment depths decrease as speed constraints decrease. With a specified depth, Figure 5.4 shows that, the total costs decrease as speed constraints increase.

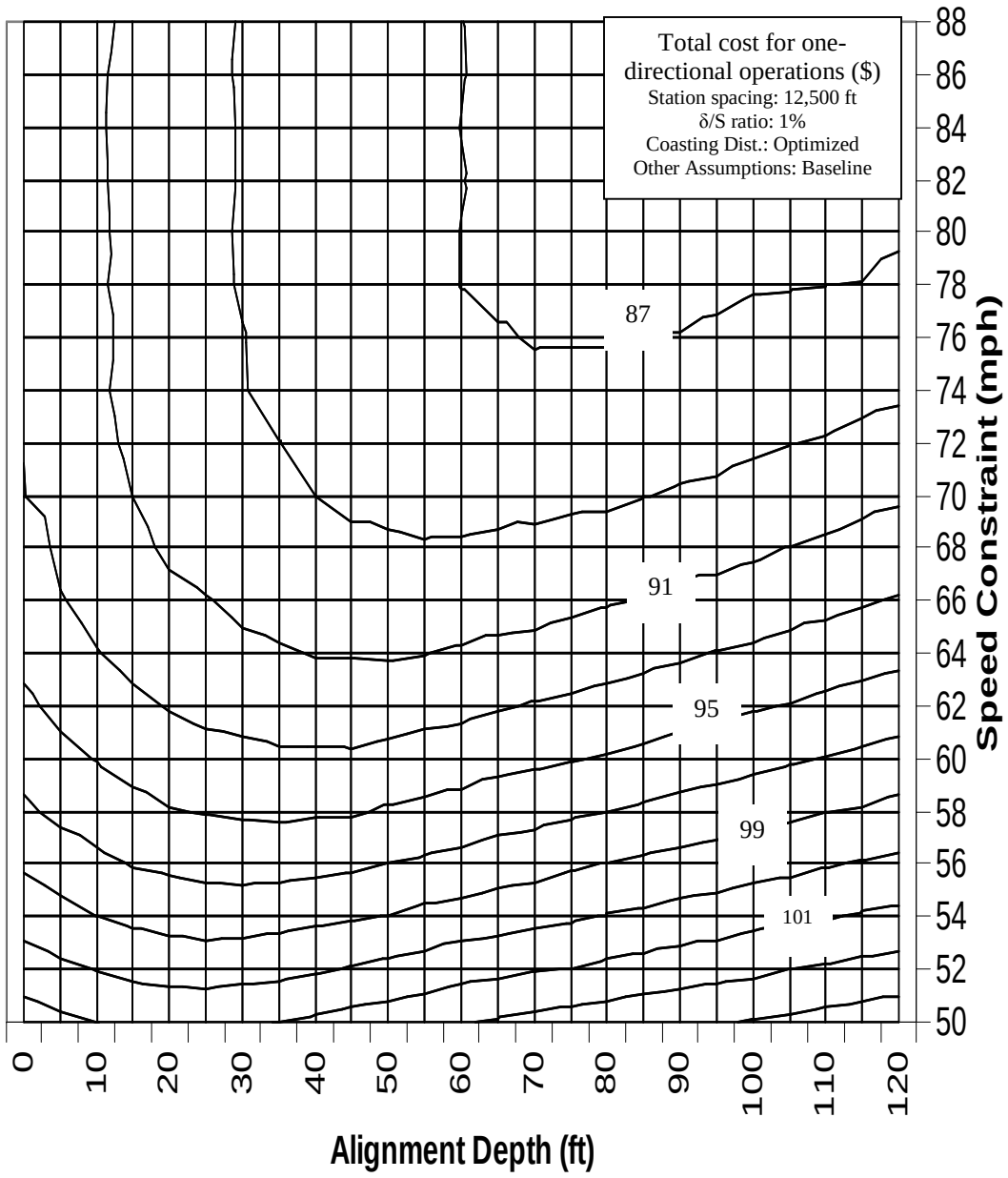

Figure 5.4 Alignment depth, speed constraint and total cost relations

Figures 5.5 and 5.6 show the relations between alignment depths, coasting distances and total costs for 75 mph and 55mph speed constraints. The diagrams show that the sensitivity of total costs to coasting distances on shallow tunnels (depth < 60 ft) are very small. Moreover, the sensitivities of total cost to alignment depth and coasting distance around the optimized point are not significant in both dimensions. However, a very sensitive area is located at upper right corner is because trains operating with long coasting distance on and deep alignments will cause significant speed drops and have disadvantages in travel time between stations. The blank upper-left areas of Figure 5.6 are cases where trains cannot reach the next station after long coasting in steep climbing sections.

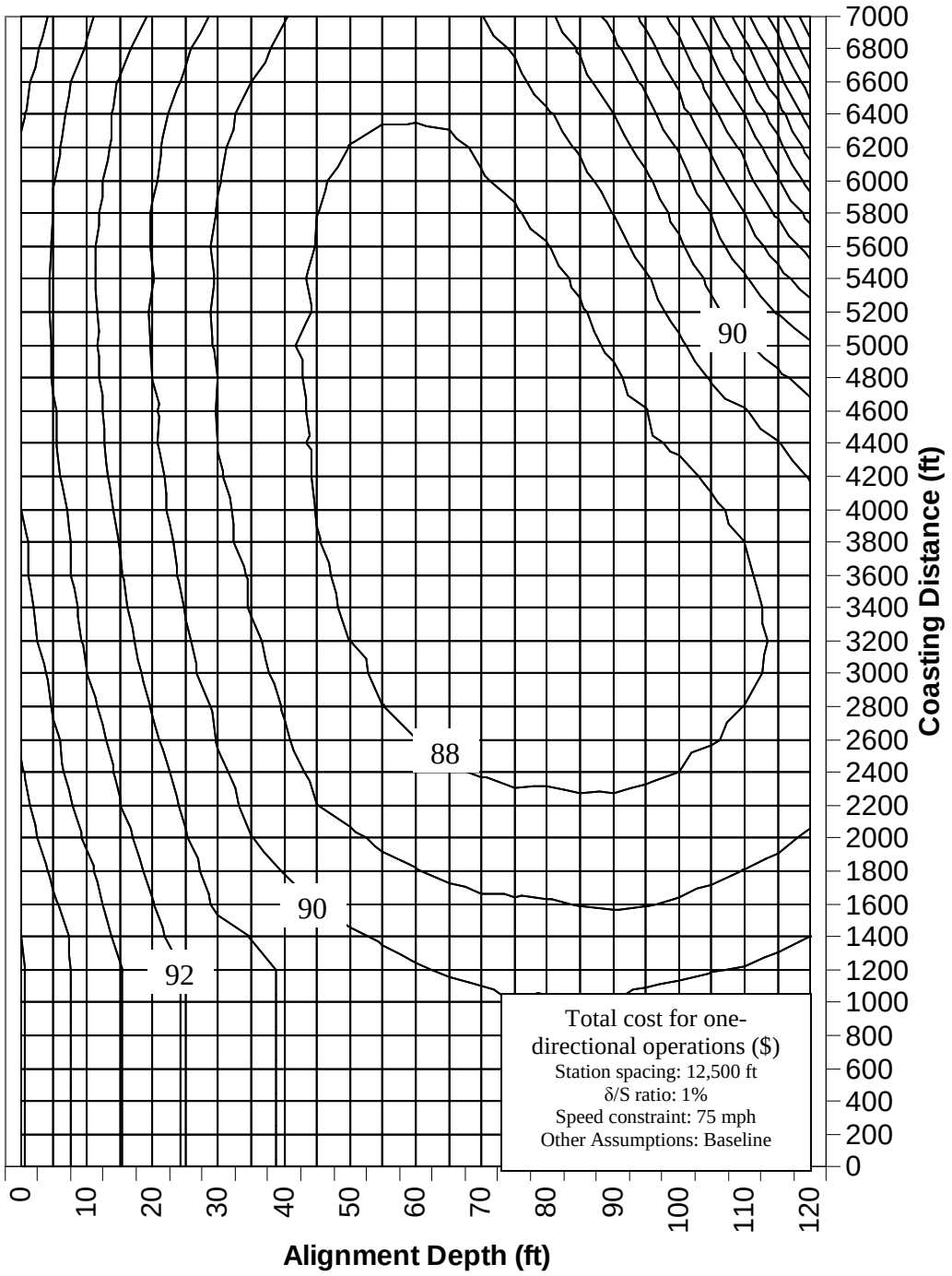

Figure 5.5 Alignment depth, coasting distance and total cost relations with a 75 mph speed constraint

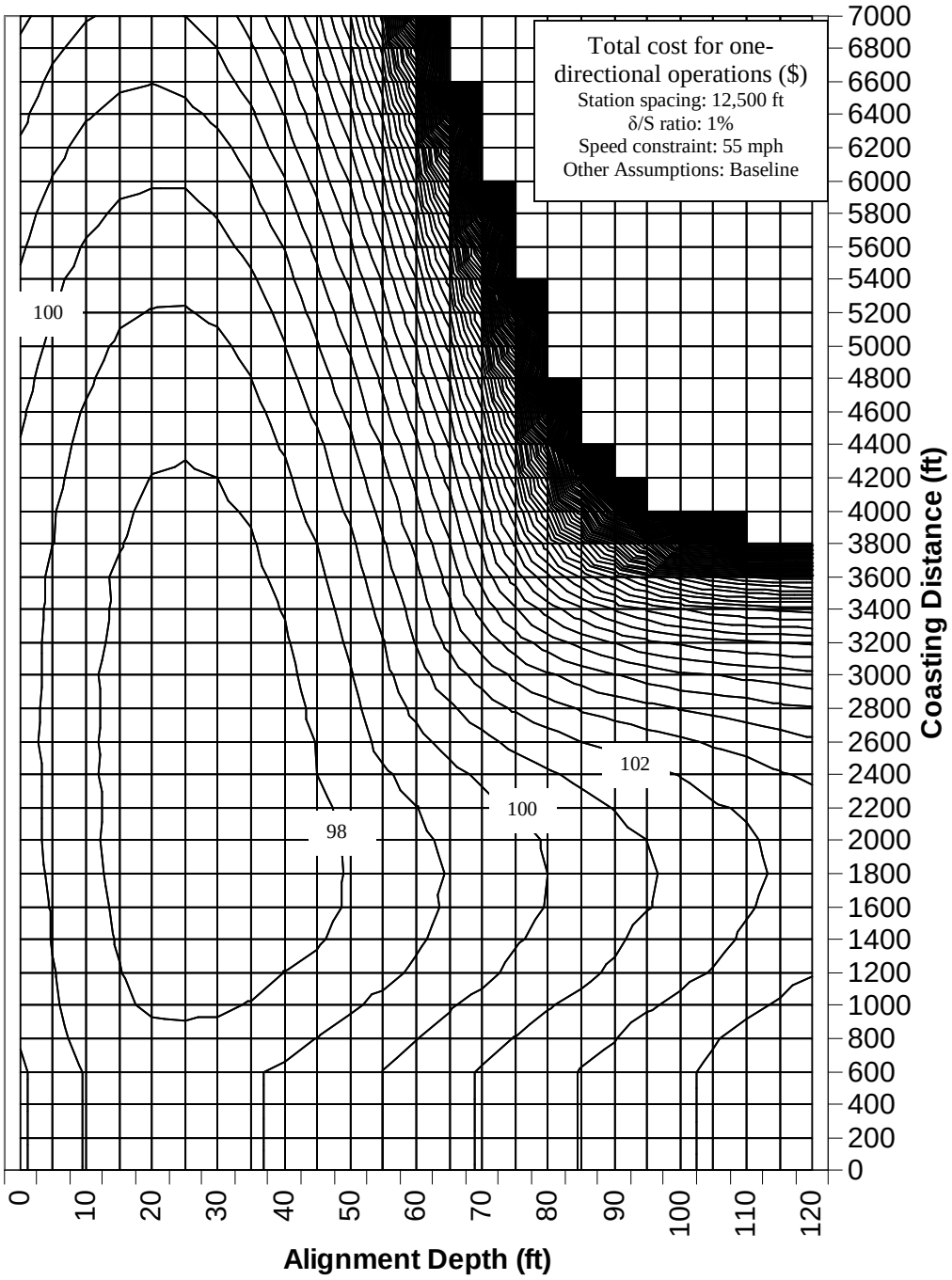

Figure 5.6 Alignment depth, coasting distance and total cost relations with a 55 mph speed constraint

5.4 Sensitivity of Optimized Alignments to User Time Value and Energy Cost

Expected changes of important parameters such as urban development and increases in energy costs within the design life of tunnels and difficulties of modifying alignments, the sensitivity of optimized alignment designs to changes in such parameters should be explored in order to avoid unsuitable alignments at later times. Figures 5.7 - 5.9 are three-dimensional relations between alignment depths, speed constraints and total costs when the passenger time value, tractive energy cost and braking energy cost are increased significantly from their baseline values. Compared with Figure 5.4, Figure 5.7-5.9 shows that the sensitivity of optimized alignments to increased passenger time value, tractive energy cost and braking energy cost are not significant. Therefore, the optimized alignments will not change significantly due to such changes in costs.

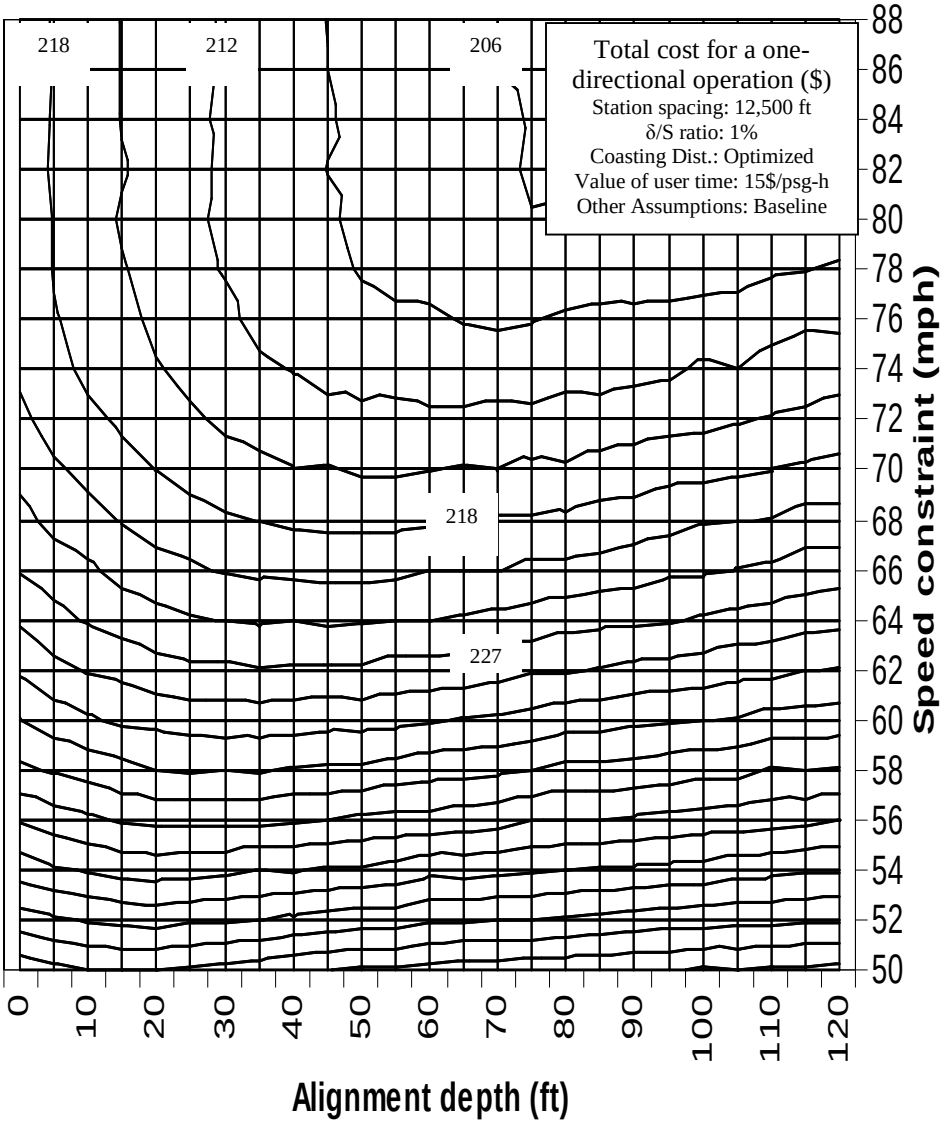

Figure 5.7 Alignment depth, speed constraint and total cost relations when the user time value is 15$/psg-hr

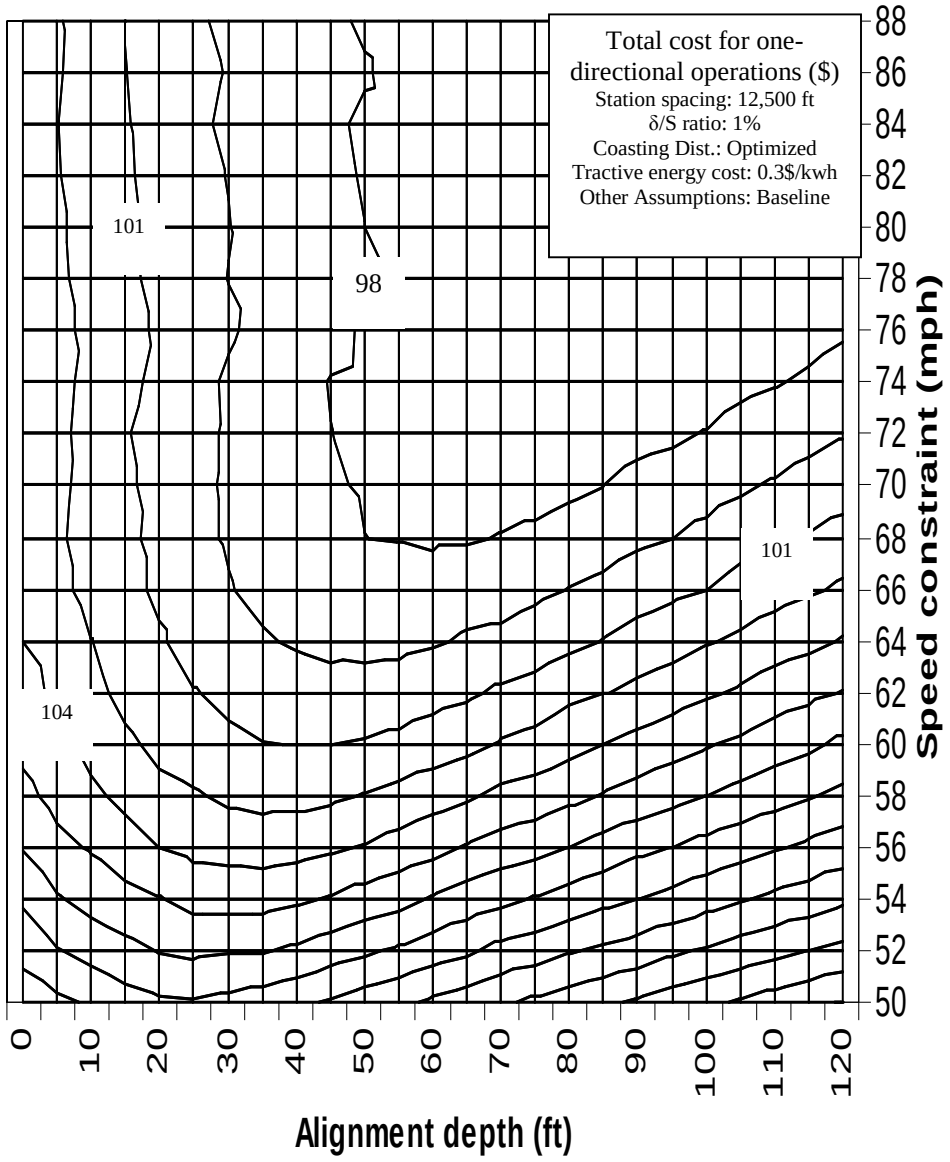

Figure 5.8 Alignment depth, speed constraint and total cost relations when the tractive energy cost is 0.3$/kwh

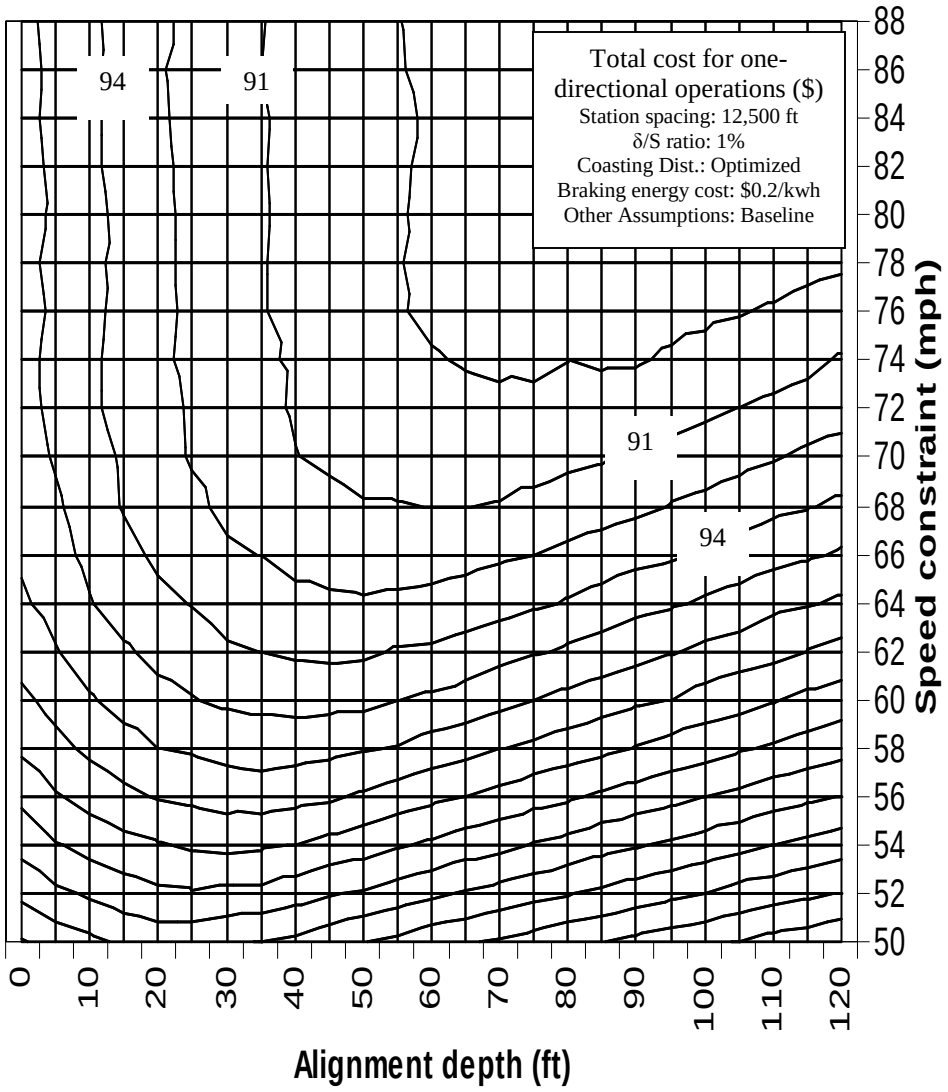

Figure 5.9 Alignment depth, speed constraint and total cost relations when the braking energy cost is 0.2$/kwh

5.5 Case Study

Benefits of using dipped track profiles between stations are estimated in this section with operating characteristics the same as WMATA METRORAIL system. The manual of design criteria (WMATA, 2001) and the annual financial report of WMATA (2002) show that the speed constrain of METRORAIL system is designed for operating safely under 75 mph. Moreover, METRORAIL trains are currently operated under 59 mph (95kph). Therefore, the use of dipped alignments with 59 mph speed constraint will be optimized. Moreover, because Figure 5.4 shows about $2 total cost saving for every one-directional operation between stations by using 20ft-depth alignment, a 20ft (3 stories) elevated station with an approaching ascending curve and a departing descending curve can be considered possible in economy and will be investigated in this case study (no consideration of construction costs in this study). Table 5.5 shows optimized results for operating with a 59 mph speed constraint inside tunnels (high air resistance). With optimized alignment (38ft-depth), A $2.80 saving in total cost for one one-directional operation between stations can be expected. Table 5.6 shows optimized solutions for operating with 59 mph speed constraint and a 20ft elevated station (S=2000ft, δ=20ft) above ground (low air resistance). A $2.22 total cost saving can be found by using elevated station sections. According to WMATA METRORAIL timetable (2003) for red line operations, there are 46,000 train operations per direction per year between METRORAIL red line stations. Therefore, the estimated annual total cost savings for a 38ft-depth double track

tunnel between stations is $257,600 and annual total cost savings for a 20ft elevated double track station is $204,240.

Table 5.5 Underground alignments optimizations with a 59mph speed constraint

Underground		Station Spacing: 8,500 ft		Station Spacing: 12,500 ft		Station Spacing: 16,500 ft	
Alignment		Level	Dipped	Level	Dipped	Level	Dipped
Optimized	S (ft)	-	3864	-	3763	-	3982
	δ (ft)	0.0	38.6	0.0	37.6	0.0	39.8
	$d_{coasting}$ (ft)	2939	2786	2927	2353	2939	2701
Performance measures	V_{max} (mph)	59	59	59	59	59	59
	L_{vmax} (ft)	2709	1721	2709	1733	2709	1711
	T (sec)	123.72	122.89	169.94	168.32	216.17	215.36
	E_t (kwh)	47.88	38.52	60.19	52.37	72.44	63.08
	E_b (kwh)	26.19	16.51	26.23	17.84	26.19	16.50
	C_t ($)	**71.66**	**68.87**	**96.62**	**93.80**	**121.57**	**118.79**
	C_t Saving ($)	-	**-2.79**	-	**-2.82**	-	**-2.78**
	C_t Saving (%)	-	**-3.89**	-	**-2.92**	-	**-2.29**

Table 5.6 Aboveground alignments optimizations with a 59mph speed constraint

Aboveground		Station Spacing: 8,500 ft		Station Spacing: 12,500 ft		Station Spacing: 16,500 ft	
Alignment		Level	Dipped	Level	Dipped	Level	Dipped
Optimized	S (ft)	-	2000	-	2000	-	2000
	δ (ft)	0	20	0	20	0	20
	$d_{coasting}$ (ft)	2634	2532	2639	2318	2634	2532
Performance measures	V_{max} (mph)	59	59	59	59	59	59
	L_{vmax} (ft)	2427	2012	2427	2012	2427	2012
	T (sec)	122.14	120.32	168.38	166.44	214.59	212.77
	E_t (kwh)	40.20	35.01	45.31	40.40	50.43	45.24
	E_b (kwh)	30.63	25.27	30.62	25.53	30.63	25.27
	C_t ($)	**70.16**	**67.94**	**94.05**	**91.83**	**117.92**	**115.70**
	C_t Saving ($)	-	**-2.22**	-	**-2.22**	-	**-2.22**
	C_t Saving (%)	-	**-3.17**	-	**-2.36**	-	**-1.89**

Chapter 6. Conclusions and Recommendations

6.1 Summary of Research Results

The primary results of this research include:

1. Development of a deterministic simulation model to investigate the rail transit vehicle movement and energy consumption under several control options and track alignment designs.
2. Analysis of the effects of using dipped vertical track alignments with baseline control options.
3. Sensitivity analysis of simulation parameters under various vertical track alignment designs.
4. Jointly optimizing of alignment designs and operating parameters.

6.2 Conclusions

1. Using dipped vertical alignments can improve the travel time, tractive energy and braking energy. Under the baseline parameters, the maximum observed saving for cases with 12,500 feet station spacing are 6.53% in travel time, 5.23% in tractive energy consumption and 23.62% in braking energy consumption.
2. For simulation cases with the same total curve length S and no speed constraints, the savings in travel time, tractive energy and braking energy are approximately proportional to the maximum depth δ.

3. Among simulation cases with fixed maximum depth δ, those with shorter total curve length S have greater savings in travel time, tractive energy and braking energy.
4. If the vehicle power-weight ratios decrease, the savings for using dipped alignments in rail transit system increase.
5. While operating outside tunnels (with low air friction), the savings for using dipped alignment in travel time and tractive energy consumption are greater.
6. Operating with constrained speeds limit the benefits from dipped alignments. Trains reaching speed limit within descending section cannot transform potential energy into kinetic energy by accelerating to higher speeds.
7. Without a speed constraint, using optimized dipped alignments can save 6.7% in total cost for a one-directional operation.
8. The optimized total cost savings in dollars are approximately equal for cases with the same low speed constraints but different station spacings.
9. With a 75 mph speed constraint, an optimized 75 feet depth alignment can save $5.4 in total cost for a one-directional operation.
10. With a 55 mph speed constraint, an optimized 27 feet depth alignment can save $2.1 in total cost for a one-directional operation.
11. The optimized total cost savings decrease as the speed constraints decrease.
12. The δ/S ratios for optimized alignments are approximately equal to 1%.
13. For optimized alignments with low speed constraint, trains reach the speed constraint at approximately the same point (L_{vmax}) where the descending curves are finished ($L_{pl}/2 + S/2$).

14. Without speed constraints, the marginal savings in total cost for unit increase in alignment depth of shallow tunnels are much higher than the marginal savings of deep alignments.
15. The sensitivities of total cost to alignment depths and coasting distances around the optimized point are not significant in both dimensions.
16. The sensitivities of total costs to coasting distances on shallow tunnels are not significant.
17. The sensitivity of optimized alignment designs to changes of user's value, energy price and braking energy cost is not significant.
18. With METRORAIL operating characteristics, the estimated annual total cost savings for a 38ft-depth double track tunnel between stations is $257,600 and annual total cost savings for a 20ft elevated double track station is $204,240.

6.3 Recommendations for Further Research

The following extensions to this work are suggested for further studies:

1. Studies of non-symmetric alignment designs

Study of stations in different level is preferred. Moreover, the vertical curves used in dipped alignment may separate into descending and climbing curves with different curvature designs to fit the best alignments in helping accelerating and in decelerating.

2. Optimizing total costs with depth-related information

In this study, the construction cost increments are assumed as zero while using deep tunnels. However, in real world, the uses of dipped alignments will cause some additional costs in constructions or in administrations. A total cost analysis and optimization that includes depth-related costs is preferred in the future study.

3. Study of above ground operations

This study shows that the marginal benefits of alignment depth changes in shallow alignments are good. Therefore, instead of using “dipped tunnel between stations”, using of “elevated stations in both ends of above ground tracks” may be studied more in the future.

4. Jointly optimizing of station spacings

Integrated study with station spacing may be introduced in the future studies. The jointly optimizing in multi-stations problems require more analyses in passenger accessing time, waiting time and station dwelling time.

5. Jointly optimizing with other design and control decisions

Joint analysis in vertical alignment design and other decisions like vehicle design are recommended in future studies.

REFERENCES

American Public Transportation Association. (2003). “Average New Rail Vehicle Costs“ [online], [cited November18, 2003]. Available from World Wide Web: (http://www.apta.com/research/stats/rail/railcost.cfm)

American Railway Engineering Association (AREA). (1984). “Manual for Railway Engineering“, Washington, D.C.

Black, A.(1995). “Urban Mass Transportation Planning“, McGraw-Hill, Inc. U.S.A.

Energy Information Administration (2003). “Average Revenue per Kilowatthour from Retail Sales to Ultimate Consumers - Estimated by Sector, by State“ [online], [cited November 18, 2003]. Available from World Wide Web:(http://www.eia.doe.gov/cneaf/electricity/epm/table5_6_a.html)

Hay, W. W. (1982). “Railroad Engineering, 2nd Ed. “, John Wiley & Sons, Inc., New York, N.Y.

Inose, J. and Ishikawa, Y. (1994) “Rises in Subway Construction Costs and Specific Examples of Reducing the Costs“, Tunnelling and ground conditions, A.A. Balkema Publishers, Brookfield, VT. 593-600.

Kikuchi, S. (1991). “A Simulation Model of Train Travel on a Rail Transit Line“, Journal of Advanced Transportation, Vol. 25, No 2, pp.211-224

Kim, D. N. and Schonfeld, P. M. (1997). “Benefits of Dipped Vertical Alignments for Rail Transit Routes“, Journal of Transportation Engineering 123, 20-27

Minciardi, R., Savio S., and Sciutto G. (1994). “Models and Tools for Simulation and Analysis of Metrorail Transit Systems“, Computers in railways IV – Volume 1, Computational Mechanics Inc., Billerica, MA. 391-402.

Press, W. H., Flannery B. P., Teukolsky S. A. and Vetterling W. T. (1989). “Numerical Recipes (Fortran Version) “, Cambridge University Press, New York, NY

Profillidis, V. A. (1995). “Railway Engineering“, Ashgate Publishing Company, Brookfield, VT.

Uher, R. A., and Sathi, N. (1983). “Reduction of Peak-Power Demand for Electric Rail Transit System“, National Cooperative Transit Research and Development Program Report 3, Transportation Research Board, Washington, D.C.

Vuchic, V. R. (1981). “Urban Public Transportation“, Prentice-Hall, Inc., Englewood Clieffs, N.J.

Washington Metropolitan Transit Authority. (2001) “Manual of Design Criteria book II“, Washington, D.C.

Washington Metropolitan Transit Authority. (2002) “Comprehensive Annual Financial Report for the Fiscal Year Earned June 30, 2002“, Washington, D.C.

Washington Metropolitan Transit Authority. (2003) “METRORAIL Timetable“, Washington, D.C.

Wright, P. H. and Ashford, N. J. (1997). “Transportation Engineering“, John Wiley & Sons, Inc., New York, N.Y.

Yu, J. G., Sturland, R. W., and Denning, L. R. (1994) “A General Motor Modeling Method for Transit System Simulation Studies“, Computers in railways IV – Volume 2, Computational Mechanics Inc., Billerica, MA. 345-348